Threshold Functions, Node Isolation, and Emergent Lacunae in Sensor Networks

Srisankar S. Kunniyur, *Member, IEEE*, and Santosh S. Venkatesh, *Member, IEEE*

***Abstract*—A geometrically random network of sensors is obtained by modeling sensors as random points in the unit disc equipped with a local sensing capability and the ability to communicate with other sensors in their vicinity. Node extinctions in the network representing the finite battery lifetimes of the sensors are modeled as a sequence of independent random variables governed by a common probability distribution parametrized by the sensing and communication radii of the sensor nodes. Following its establishment, the devolution of the network with time is characterized by the appearance first of isolated nodes, then the growth of sensory lacunae or dead spots in the sensor field, and, eventually, a breakdown in connectivity between survivors. It is shown that these phenomena occur very sharply in time, these phase transitions occurring at times characteristic of the underlying probability law governing lifetimes. More precisely, it is shown that as the number of sensors grows there exists a critical point in time determined solely by the lifetime distribution at which the number of emergent lacunae of a given size is asymptotically Poisson.**

***Index Terms*—Graph connectivity, inclusion–exclusion, phase transitions, Poisson paradigm, random graphs, sensor networks, threshold functions.**

I. Introduction

RECENT advances in sensor technology, low-power RF design and portable computing have enabled the development of densely distributed, wireless microsensor networks (cf. Chandrakasan *et al.* [1], Clare *et al.* [2], and Dong *et al.* [3]). Applications of such sensor networks include their deployment in battlefields, disaster stricken areas, environment monitoring systems and space exploration.

A characteristic feature of such networks is the untethered nature of the sensors, a consequence of which is that the battery power at each sensor becomes the primary resource constraint. Prior work on the theoretical foundations of dense sensor networks has hence focussed on the critical power required for establishing initial connectivity (at least asymptotically when there are a large number of sensors) and on the throughput that may be achieved. We discuss some of these results in the context of our model in the next section.

Manuscript received September 1, 2004; revised May 2, 2006. The work of S. S. Venkatesh was supported in part by the National Science Foundation under Grant NSF 0545015. The material in this paper was presented in part at WiOpt'04, Cambridge, U.K., Mar. 2004.

S. S. Kunniyur was with the Department of Electrical and Systems Engineering, University of Pennsylvania, Philadelphia, PA 19104 USA. He is now with Motorola Corporation, Bangalore 560093 India (e-mail: kunniyur@motorola.com).

S. S. Venkatesh is with the Department of Electrical and Systems Engineering of the University of Pennsylvania, Philadelphia, PA 19104 USA (e-mail: venkatesh@ee.upenn.edu).

Communicated by M. Médard, Associate Editor for Communications.

Digital Object Identifier 10.1109/TIT.2006.885503

Abeyant any source for power generation or battery replacement, ongoing usage of the network results inevitably in battery depletion and node failures. These networks hence exhibit a particularly transient nature with battery exhaustion causing a continual devolution and a concomitant degradation of functionality. Little is known about the dynamics of devolution of such networks and their projected lifetime. This is our focus in this paper.

Battery lifetimes in wireless sensor networks are dictated by usage patterns and the transmission power at each vertex. As batteries fail there is an inevitable devolution of the network characterized first by the appearance of isolated nodes, then by the growth of sensory lacunae or dead spots in the sensor field, and eventually a breakdown in connectivity between the surviving vertices of the network. We investigate fundamental attributes of these phenomena in a simple model of randomly deployed sensors where the battery lifetimes of the sensors are independent random variables with a common but arbitrary lifetime distribution parametrized by the power expenditure and the mean usage. In this somewhat sanitised but fundamental setting we derive sharp limit theorems characterising the time at which these phenomena make their appearance. A characteristic feature is the appearance of *phase transitions* or *threshold functions*: emergent (disruptive!) phenomena appear abruptly in a sharply concentrated time span. Our results provide explicit tradeoffs between transmission power, vertex density, and the time to emergence of various phenomena and suggest how efficient choices may be made, while providing partial answers to the following fundamental questions:

- *When does the network fail*?
- *What is the distribution of failures in the network?*

As we shall see, our results also recover the earlier known connectivity results as particular cases of a more general model. The included examples illustrate the tradeoffs in various cases.

On notation: All logarithms are to base e, $\mathbf{P}$ stands for probability measure in the underlying probability space, and $\mathbf{E}$ stands for expectation. Capitalized letters X, X_i and so on are used to denote random points in the Euclidean plane; the corresponding lower case letters x, x_i and so on denote generic points in the plane. For any point $x = (x^{(1)}, x^{(2)})$ in the plane, $|x| = \sqrt{(x^{(1)})^2 + (x^{(2)})^2}$ denotes the Euclidean norm of x.

We will use the following variants of the Landau notation. Suppose $\{f_n\}$ and $\{g_n\}$ are real sequences. As $n \to \infty$ we say that $f_n = \mathcal{O}(g_n)$ if $|f_n| \leq K|g_n|$ for some positive constant K, $f_n = \mathfrak{o}(g_n)$ if $|f_n|/|g_n| \to 0$, and $f_n \sim g_n$ if $f_n/g_n \to 1$. Note that the "big-O" and "small-o" variants in use here refer to absolute values. In consequence we will occasionally encounter an expression of the form $1 + \mathfrak{o}(1)$ for a probability—the context makes it clear that the small-o order term must in fact be

a negative, asymptotically vanishing quantity. The order terms we encounter will all be ultimately negligible and their signs will not matter. We will also commit the mild notational solecism of stringing together order relations: an expression of the form $f_n = \mathcal{O}(g_n) = \mathfrak{o}(h_n)$ means (a) that $f_n = \mathcal{O}(g_n)$ and (b) that $g_n = \mathfrak{o}(h_n)$. Of course, this also implies that $f_n = \mathfrak{o}(h_n)$ and we compact this syllogism into a single equation in the hope that there is no danger of confusion as to what is meant.

II. The Model

We begin by describing a sanitised setting in which a multihop network of functionally equivalent sensors is deployed to detect and report phenomena that may occur uniformly across a target region. Our focus will be on the graph-theoretic properties of connectivity and coverage—and their devolution in time as vertices fail—and we eschew considerations of network-specific details such as the locations of sinks and collector nodes. This setting provides perhaps the cleanest venue in which the fundamental results can be seen without obfuscation.

Our model is characterized by four elements: the nature of deployment, sensing capability, communication capability, and battery lifetimes. We outline these in turn with brief discussions and pointers to the literature.

Deployment. We consider a sensor field comprised of a circle of unit radius in which n sensors are to be dispersed. Sensors, assumed to be dimensionless nodes, are deployed randomly with locations $X_1, \ldots, X_n$ assumed to be drawn independently from the uniform distribution in the unit circle.

In an alternative model used widely in percolation theory the locations of the sensors are assumed to be governed by a two-dimensional (2-D) Poisson process in the Euclidean plane (for generalizations and extensions to stationary point processes see Meester and Roy [12]). If the Process process has intensity n/π then the restriction of the process to the unit disc yields results asymptotically equivalent to our random model via a de-Poissonization argument (cf. Penrose [14]).

Sensing capability. We suppose that each sensor can sense events within a distance $s = s_n$ from it. This is the so-called "hard-sphere" model of sensing.

Unlike transmission which is an active operation initiated by a sensor, in this context we view sensing as a largely passive operation. Sensing at larger and larger distances would imply detection of phenomena at weaker and weaker signal-to-noise ratios (SNRs) that would presumably require the implementation of more sophisticated algorithms on chip resulting in a higher power consumption. This may be taken as a justification of the hard-sphere model for sensing, at least as an initial attempt at modeling the situation, with the sensing radius $s = s_n$ of each sensor some suitably decaying function of n.

The coverage of the sensing field that is achieved depends on the sensing radius $s = s_n$. For instance, it is known that the critical sensing radius to achieve complete coverage of the unit circle is $\sqrt{(\log n)/n}$ to first order (cf. Hall [8]). If $s_n = 0$, on the other hand, we have a point sensing model where coverage in the network is only at the sensor locations. Alternatively, for a given number of sensors, one may be interested in the area of the sensor-blind region, or, yet again, in the area of the largest contiguous region that is left uncovered. Of course, many such similar questions can be posed. Coverage issues such as these have a distinguished history and have received substantial attention in the literature (Hall, *op. cit.*).

For our purposes, we place no *a priori* constraints on the choice of the sensing radius s_n but suppose that it is selected with an eye to the coverage needs at hand.

Communication capability. In addition to sensing capabilities, each sensor must be equipped with telemetry to permit it to relay information. As an abstraction of equipowered sensors equipped with isotropic antennae, we suppose that each sensor can communicate with any other sensor within a distance $c = c_n$ of it.

The power expended by a sensor during transmission is monotonically related to the communication range, typically via a power law. As the available sensor power is the critical scarce resource in this setting, in order to conserve power one can imagine a deployment where sensors utilize their neighbors to relay information through the network in a series of small hops. We will not be concerned with protocol issues here, though these can be thorny, but instead focus on how transmission power requirements may be reduced by increasing the density of sensors on the ground. Accordingly we will suppose that the communication radius $c = c_n$ is a suitably decaying function of the number of sensors n. The sensor locations hence determine a geometrically random communication network whose links are all short hops of length no more than c_n.

The key requirement in this context is that the communication radius be chosen large enough to ensure network connectivity, at least initially, immediately after deployment. As may be anticipated, the network will be connected with high probability if the communication radius c_n is sufficiently large. The most comprehensive results here are due to Penrose [13] who considers a random deployment of points in the unit square. Rephrasing his results for deployment in a square of area π puts the problem in an equivalent context to ours with a square replacing a disc of the same area. His *theorem*, in brief: *Suppose n points are distributed at random in a square of side $\sqrt{\pi}$ to form the vertices of a geometric random graph with each point communicating with others within a distance c_n of it. Let ϕ be any real constant. If*

$$c_n = \sqrt{\frac{\log n}{n} + \frac{\phi}{n} + \mathfrak{o}\left(\frac{1}{n}\right)} \tag{1}$$

then the probability that the graph is connected tends to $e^{-e^{-\phi}}$ as $n \to \infty$. In short: $\sqrt{(\log n)/n}$ is a threshold function for the radius at which the graph is connected.

The result superficially parallels the classical double exponential connectivity theorem of Erdös and Renyi [4] for the $\mathcal{G}_{n,p}$ random graph model. The difference here is that the induced geometric random graph has messy edge dependencies and thorny boundary effects at the periphery of the deployment region.

Penrose uses the Stein–Chen method of Poisson approximation by constructing a suitable coupling to prove his result.[1] In

[1]Penrose's methods extend to random deployments in the unit cube in higher dimensions though for dimensions three and higher boundary effects become dominant and explicit formulae like (1) are not available unless one finesses boundary effects by working on a torus (see Penrose [14]).

parallel work, Gupta and Kumar [7] cite similar one-way results for connectivity in a disc using tools from percolation theory.

In the sensor network context, a natural extension is to allow of the possibility of missing points or defective sensors. Yi, Wan, Li, and Frieder [18] consider a model where nodes are deployed at random in a disc, each node functional with probability p, and nonfunctional with probability $1-p$, independently of the others. They rederive Penrose's results in this setting using inclusion–exclusion arguments from the classical Poisson paradigm to show that $\sqrt{\log(n)/np}$ is a threshold function for the radius at which the graph with random vertex deletions is connected. A direct argument to this effect can also be constructed via the observation that the concentration of the binomial implies that the number of nondefective nodes is concentrated at np so that we may now leverage Penrose's connectivity result with the replacement of n, roughly speaking, by np. This tack is sketched in Kunniyur and Venkatesh [11]. Similar connectivity questions are also considered by Shakkottai, Srikant, and Shroff [15] when a certain fraction of vertices placed on a lattice are functional at any given time.

For extensions in a different direction with node connectivity driven by a mosaic process with random sets of influence, see Venkatesh [17].

To return to our model, we will take for granted that communication connectivity is a *sine qua non* and accordingly will be concerned mainly with the situation when the network of sensors is initially connected. The communication radius $c = c_n$ will hence have to be at least of the order of $\sqrt{(\log n)/n}$.

Node extinctions. Each sensor is equipped with a battery which has a finite lifetime determined by the usage patterns of the sensor and the selected communication radius. Let $T_1, \ldots, T_n$ denote the random lifetimes of the batteries of the n sensors. We will suppose that these lifetimes are independent, positive random variables with a common distribution $\mathbf{P}\{T_i \leq t\} = F(t) = F_c(t)$. *While applications in the main deal with proper distributions, our results continue to hold if the distribution F_c is defective (or improper) with positive mass at* $+\infty$. As we shall see, specific choices of defective distributions will allow us to recover all the earlier connectivity results.

As indicated in the notation, the lifetime distribution is considered to be parametrized by the communication radius supported by the battery; larger choices of c permit a smaller deployment of vertices while guaranteeing connectivity, but also deplete individual batteries faster; smaller choices of c will deplete batteries slower but require a larger number of sensor nodes to maintain connectivity, with a concomitant increase in the likelihood of node extinctions by a given time. The parametrization $F = F_c$ is hence both natural and, as we shall see in subsequent sections, essential for nontrivial results.

It will be slightly more convenient to consider the right tail of the lifetime distribution; accordingly, introduce the notation $1 - F(t) = G(t) = G_c(t)$ for the probability that the battery lifetime exceeds t. We will take the liberty of somewhat cavalierly referring to both F and G as the lifetime distribution as convenience dictates. While we make no further assumptions about the nature of the lifetime distribution G_c, for a given level of deployment, and abeyant sophisticated routing, communication over larger ranges may be expected to consume more power. Natural parametrizations may hence be expected to exhibit uniform majorizations of the form $G_{c_1} \geq G_{c_2}$ whenever $c_1 < c_2$.

The parametrization of lifetime by communication radius takes account of the fact that communication typically consumes more power than computation or sensing. While this is the main parametrization that we will consider in this paper, the notation, analysis, and results segue over smoothly to the situation where the lifetime distribution is parametrized additionally by the choice of sensing radius s with $G = G_{c,s}$. Further parametrizations by, say, a random, node-dependent usage-parameter α_i are also possible, $G = G_{c,s,\alpha_i}$. The framework easily handles cases where the α_is are independent and drawn from a common distribution. Dependencies across node usages are, however, much harder to handle and while it is likely that our main results will continue to hold under mild dependencies, significant caveats on the dependency structure will have to be spelled out.

Summary. The introduction of random lifetimes with parametrised distributions may be seen as an innovation in the basic geometric random graph model and produces several new dynamic phenomena which are the focus of this paper. Sensor failures result in an inevitable network devolution characterized first by the appearance of isolated nodes, then the formation of lacunae or sensory dead spots within the originally established network, and finally the breakdown in connectivity between survivors. Our results track this devolution in time, our main theorem demonstrating a sharp Poisson law for the first appearance of isolated nodes and lacunae. In particular, the result implies a phase transition or threshold function for the time at which coverage failure is first evidenced within the network and provides an explicit equation to be satisfied by the critical time. Apodictic support of our results and methodology is provided by the recovery of earlier connectivity results as particular cases of the model considered here.

Our basic vehicle, as in Yi *et al.* [18], is Poisson approximation via the classical method of inclusion and exclusion, though the recursive graph models introduced in our proofs and the associated bounding methods are rather different. The methods of this paper follow those outlined in Venkatesh [16]. An alternative approach is to adapt the static failure model of Yi *et al.* [18] to consider a time-inhomogeneous process with a time-dependent failure probability. Adapting Penrose's methods [13] to dynamic models is still another possibility; subsequent to the dissemination of early versions of this paper M. Francheschetti [6] has indeed kindly communicated to us that he has been able to rederive our results using Penrose's couplings in the Stein–Chen method.

III. A Poisson Law for a Devolving Geometric Random Graph

For each $r > 0$, the sensor locations induce a *geometric random graph* $\mathcal{G}_{n,r} = \mathcal{G}_{n,r}(X_1, \ldots, X_n)$ whose vertices are the points $X_1, \ldots, X_n$ in the plane. A pair of vertices (X_i, X_j) forms an edge of the graph if, and only if, $|X_i - X_j| \leq r$. If (X_i, X_j) is an edge of the graph we say that the vertices X_i and X_j are *adjacent*. The graph $\mathcal{G}_{n,r}$ hence has an intrinsically geometric character and we will refer to the X_i as vertices or points

depending on whether we wish to emphasise the graph or geometric attribute. Connectivity and coverage questions may be posed in terms of the graph $\mathcal{G}_{n,r}$ for suitable choices of $r = r_n$.

Say that a vertex X_i is *live at time t* if $T_i > t$. We also say that sensor node i is live to mean the same thing.

Definition 1: A vertex X_i of the graph $\mathcal{G}_{n,r}$ is *isolated at time t* if there are no live vertices X_j adjacent to X_i at time t in $\mathcal{G}_{n,r}$.

In other words, vertex X_i in $\mathcal{G}_{n,r}$ is isolated at time t if $T_j \leq t$ for every vertex X_j adjacent to X_i in $\mathcal{G}_{n,r}$. If a vertex is isolated in $\mathcal{G}_{n,c}$ then phenomena detected by the node at that location cannot be communicated to the rest of the network; likewise, if a vertex is isolated in $\mathcal{G}_{n,s}$ then no node in the network at large can sense phenomena at that node's location. Thus, if vertex X_i is isolated in $\mathcal{G}_{n,\max\{c,s\}}$ at time t then the network at large would thereafter be sensorily blind to phenomena at the location of node i. The conclusion is slightly conservative as it ignores the condition of node i itself and we will refine this picture of sensory isolation a little; but first, a generalization expanding the idea of geometric isolation from a point to a disc.

For $\ell \geq 0$, write $\mathbb{D}(\ell; x) = \{y : |y-x| \leq \ell\}$ for the Euclidean disk of radius ℓ centered at x and, in a slight abuse of notation, for any $0 \leq \ell_1 < \ell_2$, write $\mathbb{D}(\ell_1, \ell_2; x) = \mathbb{D}(\ell_2; x) \setminus \mathbb{D}(\ell_1; x) = \{ y : \ell_1 < |y - x| \leq \ell_2\}$ for the annulus between the discs of radius ℓ_1 and ℓ_2 centered at x. To keep notation unburdened we will write $\mathbb{D}_i(\ell) = \mathbb{D}(\ell; X_i)$ for the disc of radius ℓ centered at vertex X_i and, likewise, $\mathbb{D}_i(\ell_1, \ell_2) = \mathbb{D}(\ell_1, \ell_2; X_i)$ for annuli centered at vertex X_i.

Definition 2: The disc $\mathbb{D}_i(\ell)$ is *isolated at time t in* $\mathcal{G}_{n,r}$ if the annulus $\mathbb{D}_i(\ell, \ell + r)$ contains no live vertices at time t.

The case $\ell = 0$ returns us to the notion of an isolated vertex. Lacunae or sensory dead spots at and in the vicinity of network nodes emerge with the appearance of isolated discs centered at node locations: arguing as before, if $\mathbb{D}_i(\ell)$ is isolated at time t in $\mathcal{G}_{n,\max\{c,s\}}$ then the network at large will be unable to register phenomena originating subsequently in the disc of radius ℓ centered at the location of node i.

We are interested in what can be said about the distribution of the number of isolated vertices and discs of a given size, and their evolution in time for a given lifetime distribution $G(t) = G_c(t) = \mathbf{P}\{T_i > t\}$. Write ${}^{\ell}N(t; r, c)$ for the number of isolated discs of radius ℓ centered at network vertices at time t in the graph $\mathcal{G}_{n,r}$. In particular, ${}^{0}N(t; r, c)$ is the number of isolated vertices at time t in $\mathcal{G}_{n,r}$. Our main result asserts a sharp limit theorem for ${}^{\ell}N(t; r, c)$ in a suitable range.

Main Theorem: Let λ be any fixed positive constant. Suppose ℓ_n, r_n, c_n, and t_n are nonnegative sequences and let

$$R_n = \sqrt{2\ell_n r_n + r_n^2}.$$

Suppose these sequences satisfy the asymptotic properties

$$R_n = \mathfrak{o}\left(\frac{\log n}{\sqrt{n}}\right)$$

and

$$R_n^2 G_{c_n}(t_n) = \frac{1}{n}\log\frac{n}{\lambda} + \mathfrak{o}\left(\frac{1}{n}\right) \tag{2}$$

as $n \to \infty$. Then ${}^{\ell_n}N(t_n; r_n, c_n)$ converges in distribution to the Poisson distribution with mean λ. More specifically,

$$\mathbf{P}\left\{{}^{\ell_n}N(t_n; r_n, c_n) = m\right\} \to e^{-\lambda}\lambda^m/m! \qquad (n \to \infty)$$

for every fixed nonnegative integer m.

Remarks: Two remarks are in order before we proceed.

1) The choice of the disc of unit radius as the sensor field saves a little in the notation. If the sensor field is a disc of radius M we only need to replace the second equation in (2) by $R_n^2 G_{c_n}(t_n) = \frac{M^2}{n}\log\frac{n}{\lambda} + \mathfrak{o}(\frac{1}{n})$. As will be apparent from the proof, matters do not change materially for a general sensor field. If the field is geometrically nice and has area $\mathfrak{A}$, the theorem will hold with the second equation in (2) replaced by $R_n^2 G_{c_n}(t_n) = \frac{\mathfrak{A}}{\pi n}\log\frac{n}{\lambda} + \mathfrak{o}(\frac{1}{n})$. Here "niceness" means roughly that the perimeter of the field is not dominant vis à vis the interior.
2) The dependence of ${}^{\ell_n}N(t_n; r_n, c_n)$ on c_n is implicit through the parameterization of the lifetime distribution $G(t) = G_{c_n}(t)$ by the communication radius c_n. As will become clear in the examples below, this parametrization is both natural and critical.

A large number of interesting results arise out of the MAIN THEOREM and we outline these in a series of corollaries in the next section.

IV. PHASE TRANSITIONS: FROM CONNECTIVITY TO LACUNAE

For the specific case of isolated vertices in the communication graph $\mathcal{G}_{n,c}$, we obtain the following useful specialization by setting $\ell_n = 0$ and $r_n = c_n$ in the MAIN THEOREM.

Corollary 1 (Isolated Vertices): Suppose the sequences c_n and t_n vary with n such that

$$c_n = \mathfrak{o}\left(\frac{\log n}{\sqrt{n}}\right)$$

and

$$c_n^2 G_{c_n}(t_n) = \frac{1}{n}\log\frac{n}{\lambda} + \mathfrak{o}\left(\frac{1}{n}\right) \tag{2'}$$

as $n \to \infty$. Then the number of isolated vertices at time t_n in the graph $\mathcal{G}_{n,c_n}$ converges in distribution to the Poisson distribution with mean λ and *a fortiori* the probability that there are no isolated vertices in the graph $\mathcal{G}_{n,c_n}$ tends to $e^{-\lambda}$.

A further specialization leads to the basic connectivity result in geometric random graphs. Suppose $F^{(1)}$ is the (trivial) defective distribution with all its mass at $+\infty$, that is to say, $F^{(1)}(t) = 0$ (equivalently, $G^{(1)}(t) = 1 - F^{(1)}(t) = 1$) for all t with the measure corresponding to $F^{(1)}$ placing mass 1 at the point $+\infty$ of the extended real line. Battery lifetimes are infinite under this distribution and the network, once established, persists indefinitely, unchanged from its incarnation at $t = 0$.

Corollary 2 (Threshold Radius): Suppose vertices in the graph $\mathcal{G}_{n,c_n}$ are never extinguished, that is to say, they have lifetimes governed by the defective distribution $F^{(1)}$. Suppose c_n varies with n so that

$$c_n = \sqrt{\frac{1}{n}\log\frac{n}{\lambda} + \mathfrak{o}\left(\frac{1}{n}\right)} \tag{1'}$$

as $n \to \infty$. Then the number of isolated vertices in $\mathcal{G}_{n,c_n}$ converges to the Poisson distribution with mean λ.

As in the Erdös–Rényi result for connectivity in the classical random graph $\mathcal{G}_{n,p}$, the primary mechanism for breakdown in connectivity in the geometric random graph $\mathcal{G}_{n,c_n}$ is the presence of isolated vertices. A Peierls argument following Penrose [13] formalizes this idea and allows us now to obtain the fundamental connectivity *theorem*: *If c_n satisfies* (1′) *then the probability that the geometric random graph $\mathcal{G}_{n,c_n}$ is initially connected tends to $e^{-\lambda}$ for any lifetime distribution without mass at zero*. A comparison with (1) shows that, with $\lambda = e^{-\phi}$, this is the analogue for deployment in the unit disc of Penrose's result for deployments in a square of side $\sqrt{\pi}$. The main difficulty in going from the square to the circle is that the boundary effects become much more unpleasant for the disc but, as for the square, ultimately prove negligible in two dimensions. For more discussion and extensions, see Venkatesh [16].

Another specialization allows us to recover the result of Yi *et al.* [18] for connectivity when a certain fraction of nodes is nonfunctional. Write $F^{(0)}$ for the distribution concentrated at the origin: $F^{(0)}(t) = 1$ for $t \geq 0$. The (proper) distribution $F^{(0)}$ corresponds to the trivial situation where all lifetimes are identically zero. For any $0 < p \leq 1$, let $F^{(p)} := pF^{(1)} + (1-p)F^{(0)}$ be the defective mixture of $F^{(1)}$ and $F^{(0)}$. Then $F^{(p)}(t) = 1-p$ (equivalently, $G^{(p)}(t) = p$) for $t \geq 0$ with the measure corresponding to $F^{(p)}$ placing a mass of p at the point $+\infty$. Under the defective lifetime distribution $F^{(p)}$, initially each node is nonfunctional with probability $1-p$ and functional with probability p, with functional nodes persisting for all time thereafter.

Corollary 3 (Defective Nodes): Suppose vertices in the graph $\mathcal{G}_{n,c_n}$ have a lifetime distribution governed by the defective distribution $F^{(p)}$ for some $0 < p \leq 1$. Suppose c_n varies with n so that

$$c_n = \sqrt{\frac{1}{np}\log\frac{n}{\lambda} + \mathfrak{o}\left(\frac{1}{n}\right)} \qquad (1'')$$

as $n \to \infty$. Then the number of isolated vertices in $\mathcal{G}_{n,c_n}$ converges to the Poisson distribution with mean λ.

Another deployment of a Peierls argument recovers the result of Yi *et al.* [18] for connectivity in the presence of defective nodes: *If c_n satisfies* (1″) *then, under the lifetime distribution $F^{(p)}$, the probability that $\mathcal{G}_{n,c_n}$ is connected tends to $e^{-\lambda}$.*

Observe that the conditions embodied in (2′) restrict c_n to asymptotic orders between $\sqrt{(\log n)/n}$ and $(\log n)/\sqrt{n}$ (as $G_c(t)$ is majorized by 1 for all c). The order of the lower bound cannot be improved as a radius of order at least $\sqrt{(\log n)/n}$ is requisite for connectivity in the communication graph via the remark following Corollary 2; in particular, the connectivity region is solidly within the province of the theorem. As we shall see in the course of the proof, the upper bound for the rate for c_n embodied in the latter condition also turns out to be best possible for the stated results to hold; more generally, *the rates embodied in* (2) *are essentially best possible*.

For a given (proper) lifetime distribution $G = G_{c_n}$, as time advances the graph gradually devolves from conditions of initial connectivity to the first appearance of isolated vertices and then isolated discs. Under the conditions of the theorem, at the critical time $t = t_n$, the probability that there are no isolated discs tends to $e^{-\lambda}$ whence the probability that there are one or more isolated discs tends to $1 - e^{-\lambda}$. The choice of the positive λ will determine which of the two situations is likely to prevail: a small λ makes it unlikely that any discs are isolated in the time frame of interest while a large λ makes it rather likely that discs will become isolated. For a given parametric family of distributions $G(t) = G_{c_n}(t)$, the conditions (2), (2′) implicitly determine the critical value of time $t = t_n$ at which there is a threshold function (or *phase transition*) and isolated discs (vertices) begin to appear.

Consider, for instance, a random deployment of sensors in a circular sensor field of radius M. In this case, the second condition in (2′) is replaced by (see the remarks following the MAIN THEOREM)

$$G_{c_n}(t_n) = \frac{M^2}{nc_n^2}\log\frac{n}{\lambda} + \mathfrak{o}\left(\frac{1}{nc_n^2}\right).$$

For a given distribution, the above equation can in principle be inverted to determine the critical time t_n at which isolated vertices ($\ell_n = 0$) appear in the communication graph $\mathcal{G}_{n,c_n}$ though the details depend upon the choice of distribution. Some illustrative examples may help flesh out the asymptotics.

Suppose first that the lifetime distribution G_{c_n} is memoryless. The parametrization with c_n may be captured by modeling increased drain on a battery due to larger communication radii via a power law in c_n in the exponent. A fourth-power law in c_n would connote, for example, adverse conditions and a high-drain situation. Routine calculations now allow us to invert the above equation for $G_{c_n}(t_n)$ with the result claimed below verifiable by direct substitution.

Corollary 4 (High-Drain Exponential): Suppose the battery lifetime has the memoryless, high-drain distribution $G_{c_n}(t) = e^{-\alpha c_n^4 t}$ where the positive α represents a mean usage parameter. If c_n has asymptotic order between $\sqrt{(\log n)/n}$ and $(\log n)/\sqrt{n}$ then at time

$$t_n = \frac{1}{\alpha c_n^4}\left[\log\left(nc_n^2\right) - \log\log n - 2\log M + \frac{\log\lambda}{\log n} + \mathfrak{o}\left(\frac{1}{\log n}\right)\right]$$

the number of isolated vertices in the graph $\mathcal{G}_{n,c_n}$ is asymptotically Poisson with mean λ.

For example, if the communication radius is at the critical range required for connectivity, say $c_n = M\sqrt{\frac{\log n + \kappa}{n}}$ for a suitably large positive κ, then $t_n \sim n^2\log(\lambda e^{\kappa})/\alpha M^4\log^3 n$ so that the critical range of time at which isolated vertices begin to appear for the first time is of the order of $n^2/\log^3 n$. If the communication radius is super-critical, however, a similar analysis shows that isolated vertices crop up somewhat earlier in time. If, for instance, $c_n = \sqrt{\log^2(n)/n\log\log n}$ then the critical range of time is asymptotic to $n^2(\log\log n)^3/\alpha\log^4 n$ which is $\mathfrak{o}(\frac{n^2}{\log^3 n})$. Thus, a supercritical communication radius results in an earlier appearance of isolated vertices in accordance with naive expectation though the explicit threshold function for the time to emergence of isolated vertices quantifies the role of the

battery power. The next example illustrates however that quite the reverse can occur. With a memoryless distribution for battery lifetimes, as above, suppose now that the lifetime dependence on power varies quadratically as would be the case in a "clean" environment.

Corollary 5 (Low-Drain Exponential): Suppose the battery lifetime has the memoryless, low drain distribution $G_{c_n}(t) = e^{-\alpha c_n^2 t}$ where the positive α again represents a mean usage parameter. If c_n has asymptotic order between $\sqrt{(\log n)/n}$ and $(\log n)/\sqrt{n}$ then at time

$$t_n = \frac{1}{\alpha c_n^2}\left[\log\left(nc_n^2\right) - \log\log n - 2\log M + \frac{\log\lambda}{\log n} + \mathfrak{o}\left(\frac{1}{\log n}\right)\right]$$

the number of isolated vertices in the graph $\mathcal{G}_{n,c_n}$ is asymptotically Poisson with mean λ.

With initial critical connectivity $c_n = M\sqrt{\frac{\log n+\kappa}{n}}$, the threshold function for the appearance for isolated vertices is asymptotic to $t_n \sim n\log(\lambda e^{\kappa})/\alpha M^2\log^2 n$ which is of the order of $n/\log^2 n$. For super-critical initial connectivity $c_n = \sqrt{\log^2(n)/n\log\log n}$ the critical range of time is now asymptotic to $n(\log\log n)^2/\alpha\log^2 n$ which increases faster than $n/\log^2 n$. In this model, a supercritical initial radius for connectivity ensures a longer period of time before the first appearance of isolated vertices. *Thus, while a lower density of vertices (near the critical number needed for connectivity) is preferred when the drain is high, quite the reverse is true when the drain is low.*

Karamata's [9] theory of regularly varying functions yields a large range of useful heavy-tailed distributions as candidate lifetime distributions. Suppose $\sigma < 0$. We say that G *is regularly varying with exponent* σ if $G_{c_n}(t) \sim \mu(c_n)t^{\sigma}$ as $t \to \infty$ for some positive, monotonically decreasing function μ.

Corollary 6 (Regular Variation): If $G_{c_n} \sim \mu(c_n)t^{\sigma}$ is regularly varying with exponent σ then the critical range of t_n around which isolated vertices start to appear in the communication graph is

$$t_n \sim \left(\frac{M^2}{nc_n^2\mu(c_n)}\log\frac{n}{\lambda}\right)^{\frac{1}{\sigma}}.$$

The critical communication radius for connectivity, $c_n \sim M\sqrt{\log(n)/n}$, buys us little here unless $\mu(r)$ decreases to zero as $r \to 0$. If the communication radius is supercritical, for example $c_n \sim \sqrt{\log^2(n)/n\log\log n}$, then extinction occurs much faster at $t_n \sim (\frac{M^2\log\log n}{\mu(c_n)\log n})^{\frac{1}{\sigma}}$.

Returning to a general lifetime distribution G_{c_n}, as time proceeds isolated vertices appear and then give way in turn to isolated discs. As we've seen, the isolation of $\mathbb{D}_i(\ell)$ in $\mathcal{G}_{n,\max\{c,s\}}$ implies a sensory lacuna or dead spot centered at vertex X_i. A slightly more precise picture emerges if we consider the health of the sensory nodes inside the disc $\mathbb{D}_i(\ell)$ as well.

In general, the presence of a sensory dead spot of radius ℓ centered at vertex X_i implies both a cessation of sensing from without the disc *and* a cessation of communication from within the disc. More formally, there will be a sensory dead spot of radius ℓ centered at vertex X_i at time t if the following two conditions are jointly satisfied at that time.

1) No live vertex external to the disc $\mathbb{D}_i(\ell)$ has a sensory region that intersects the disc. For this condition to hold it is necessary and sufficient that there be no live vertices in the annulus $\mathbb{D}_i(\ell,\ell+s)$.
2) No live vertex within the disc $\mathbb{D}_i(\ell)$ has a communication pathway to the network at large. For this condition to hold it suffices if there are no live vertices in the disc $\mathbb{D}_i(\ell)$ or, alternatively, if there are no live vertices in the annulus $\mathbb{D}_i(\ell,\ell+c)$.

These considerations suggest the following formal characterization of lacunae in the network.

Definition 3: We say that there is a *sensory lacuna of radius ℓ centered at vertex X_i at time t* if the following two conditions are satisfied at time t: 1) the annulus $\mathbb{D}_i(\ell,\ell+s)$ contains no live vertices; and 2) at least one of the disc $\mathbb{D}_i(\ell)$ or the annulus $\mathbb{D}_i(\ell,\ell+c)$ contains no live vertices.

The latter condition is slightly conservative as it is only really requisite that there are no live vertices external to $\mathbb{D}_i(\ell)$ which are within a distance c of any live vertex in $\mathbb{D}_i(\ell)$ to make communication out of the disc $\mathbb{D}_i(\ell)$ impossible. However, at critical communication connectivity and beyond, the density of nodes on the ground is such that node separations are no more than the order of $n^{-1/2}$; the geometrically regular picture of circles and annuli of influence that is conjured up by the definition is both analytically convenient and not far removed from the reality on the ground.

Let $u(x)$ denote the unit step function taking value 1 for $x \geq 0$ and value 0 for $x < 0$. Define

$$\begin{aligned} P_n &= P_n(\ell,s,c,t) \\ &= e^{-n[(\ell+\max\{s,c\})^2-\ell^2]G_c(t)} \\ &\quad + (1-G_c(t))\left\{e^{-n(\ell+s)^2G_c(t)} - e^{-n(\ell+c)^2G_c(t)}\right\}u(c-s). \end{aligned} \quad (3)$$

We will see that if $\ell_n^2+s_n^2+c_n^2 = \mathfrak{o}(\frac{\log^2 n}{n})$ then the probability that there is a lacuna of radius ℓ_n at any given network vertex at time t_n is asymptotic to $P_n(\ell_n,s_n,c_n,t_n)$. As a consequence of the proof of the MAIN THEOREM we then quickly obtain a Poisson law for the number of lacunae and thence a phase transition for the time to their emergence.

Corollary 7 (Lacunae): Suppose $\ell_n^2+s_n^2+c_n^2 = \mathfrak{o}(\frac{\log^2 n}{n})$. If $P_n(\ell_n,s_n,c_n,t_n) \sim \lambda/n$ then the number of lacunae of radius ℓ_n centered at network vertices at time t_n converges in distribution to the Poisson distribution with mean λ.

Some examples may help to make the formidable-looking asymptotic condition intelligible.

Example 1: Point lacunae at network vertices. Setting $\ell = 0$ in (3) yields

$$\begin{aligned} P_n &= e^{-n(\max\{s,c\})^2G_c(t)} \\ &\quad + \left[e^{-ns^2G_c(t)} - e^{-nc^2G_c(t)}\right]u(c-s) \\ &= e^{-ns^2G_c(t)} \end{aligned}$$

for all $s \geq 0$. It follows that the number of point lacunae satisfy an asymptotic Poisson law with mean λ if $e^{-ns_n^2 G_{c_n}(t_n)} \sim \lambda/n$. A comparison with (2), (2′) shows that this is equivalent asymptotically to the problem of isolated vertices in the graph $\mathcal{G}_{n,s_n}$. The critical time t_n at which point lacunae first emerge may now be determined as in Corollaries 4–6. □

Example 2: Lacunae over regions of nodal coverage. With $\ell = s$ in (3) we obtain

$$P_n = e^{-n[(s+c)^2 - s^2]G_c(t)} + (1 - G_c(t)) \times \left\{ e^{-4ns^2 G_c(t)} - e^{-n(s+c)^2 G_c(t)} \right\}$$

when $s \leq c$, while

$$P_n = e^{-3ns^2 G_c(t)}$$

when $s > c$. For definiteness, now suppose $s_n = \alpha c_n$ for some $\alpha > 0$. If $0 < \alpha < 1/(\sqrt{5} - 1)$ then we are in the regime $s_n \leq c_n$ and it is easy to see that $P_n \sim (1 - G_{c_n}(t_n))e^{-4ns_n^2 G_{c_n}(t_n)}$ as the other two exponential terms are subdominant (bear in mind that communication connectivity requirements allied with the conditions embodied in (2) will force $1 - G_{c_n}(t_n)$ to be of order at least $1/\log n$); if $\alpha = 1/(\sqrt{5} - 1)$ then $P_n \sim (2 - G_{c_n}(t_n))e^{-4ns_n^2 G_{c_n}(t_n)}$; if $\alpha \geq 1$ then $P_n = e^{-3ns_n^2 G_{c_n}(t_n)}$. Thus, P_n increases asymptotically from $(1 - G_{c_n}(t_n))e^{-4ns_n^2 G_{c_n}(t_n)}$ to $e^{-3ns_n^2 G_{c_n}(t_n)}$ as α increases. The corresponding threshold functions for t_n may be determined again as in Corollaries 4–6. As may have been anticipated, the time to appearance of lacunae decreases monotonically as α, hence also s_n, increases; our results quantify the exact relationship. □

V. Proofs

We require the following elementary inequalities; the proofs follow from routine Taylor arguments and are omitted.

Lemma 1: Bounds for elementary functions.

a) Arc sine: $\arcsin x \geq x$ for $0 \leq x \leq 1$ and $\arcsin x \leq x + x^3 \leq 2x$ for $0 \leq x \leq 0.6083$.
b) Logarithm: $\log(1 - x) = -x + \mathcal{O}(x^2)$ as $x \to 0$.
c) Exponential: $1 + x \leq e^x$ for all x and $e^x = 1 + x + \mathcal{O}(x^2)$ as $x \to 0$. In particular, $(1 - x)^a = 1 - ax + \mathcal{O}(x^2)$ as $x \to 0$ for every real a.

Refinements of standard inclusion–exclusion arguments go by the collective name of Bonferroni's inequalities (cf. Feller [5]). We will use the following variant.

Suppose $A_1, \ldots, A_n$ are events in a probability space and let P_m denote the probability of the event that exactly m of the A_i occur. The inclusion–exclusion formula then gives us the explicit result

$$P_m = \sum_{k=0}^{n-m} (-1)^k \binom{m+k}{m} S_{m+k} \tag{4}$$

where S_k is the sum of all the probabilities of conjunctions of the events A_i, k at a time. It will be convenient to introduce the notation

$$f_m(K) = \sum_{k=0}^{K-1} (-1)^k \binom{m+k}{m} S_{m+k}$$

for the truncated sums of the inclusion–exclusion formula. Clearly, $f_m(n - m + 1) = P_m$, but much more can be said.

Lemma 2: The truncated sums $f_m(K)$ form an increasingly fine series of approximations to P_m and bound P_m from below when K is even and from above when K is odd. More precisely, the approximation error $P_m - f_m(K)$ has the sign $(-1)^K$ of the first neglected term in the inclusion–exclusion formula (4) and is bounded in absolute value by that term.

We omit the standard proof.

We now turn to the proof of the Main Theorem. The specification of the lacuna radius ℓ_n plays no essential role in the structure of the proof of the Main Theorem, though of course the particular choice affects the critical time t_n at which isolated discs $\mathbb{D}_i(\ell_n)$ first emerge in the graph $\mathcal{G}_{n,r_n}$. We simplify presentation accordingly by considering first the case $\ell_n = 0$. The setting is now that of isolated vertices in the graph $\mathcal{G}_{n,r_n}$ and with $R_n = r_n$ the conditions (2) become

$$r_n = \mathfrak{o}\left(\frac{\log n}{\sqrt{n}}\right) \quad \text{and} \quad r_n^2 G_{c_n}(t_n) = \frac{1}{n}\log\frac{n}{\lambda} + \mathfrak{o}\left(\frac{1}{n}\right) \tag{2″}$$

as $n \to \infty$. Before proceeding, it will be useful to observe that these conditions imply the asymptotic order relations

$$e^{-nr_n^2 G_{c_n}(t_n)} \sim \frac{\lambda}{n}$$
$$nr_n^3 G_{c_n}(t_n) = \mathcal{O}(r_n \log n) = \mathfrak{o}\left(\frac{\log^2 n}{\sqrt{n}}\right),$$
$$nr_n^4 G_{c_n}^2(t_n) = \mathcal{O}\left(\tfrac{\log^2 n}{n}\right).$$

The Main Theorem specialized to this setting says that under the conditions (2″) the number of isolated vertices at time t_n in the graph $\mathcal{G}_{n,r_n}$ converges in distribution to the Poisson with mean λ.

As will become apparent, the proof for the general case will carry through with little more than the systematic replacement of r_n by $R_n = \sqrt{2\ell_n r_n + r_n^2}$ in the following development.

To keep the notational mess under control, we will from now on, suppress subscripts when it is possible to do so without confusion; for instance, we write $r = r_n, t = t_n$, and $G(t) = G_{c_n}(t_n)$. We also suppress the roles of r_n and c_n and write simply ${}^0N(t) = {}^0N(t_n; r_n, c_n)$ for the number of isolated vertices at time $t = t_n$ in the graph $\mathcal{G}_{n,r_n}$.

It will be useful to set up some additional notation at this stage. As before, write ${}^0L_i(t)$ for the event that vertex X_i is isolated by time $t = t_n$ in the graph $\mathcal{G}_{n,r_n}$ and, in an extension of this notation, ${}^0L_{i_1,\ldots,i_k}(t)$ for the event that vertices $X_{i_1}, \ldots, X_{i_k}$ are all isolated by time t. Write ${}^0P(t) = \mathbf{P}({}^0L_i(t))$ for the probability that vertex X_i is isolated by time t; by symmetry, this probability does not depend

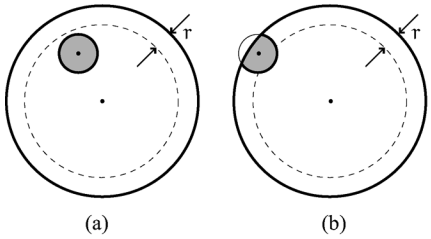

Fig. 1. Two cases for the region of visibility (shown shaded). (a) X_i lies in the interior of the unit circle. (b) X_i lies in an annulus of width r at the boundary of the unit circle.

upon the choice of i though there is of course an implicit dependence on n. It follows that $\frac{1}{n}\mathbf{E}\{{}^0N(t)\} = {}^0P(t)$.

It will be natural to break up the proof of the MAIN THEOREM under the conditions (2″) into three stages. We begin by proving the following proposition.

Proposition 1: Vertex isolations are rare, or more precisely, ${}^0P(t) \sim \lambda/n$ as $n \to \infty$.

Moreover, we show the following.

Proposition 2: Vertex isolations are weakly asymptotically independent, or more precisely

$$\mathbf{P}\left({}^0L_{i_1,\ldots,i_k}(t)\right) \sim [{}^0P(t)]^k \sim \frac{\lambda^k}{n^k} \qquad (n \to \infty)$$

for every fixed positive integer k.

And to finish up, we show that the conclusion of the MAIN THEOREM follows.

Proposition 3: Aberrant vertices are trapped in a Poisson sieve, or more formally,

$$\mathbf{P}\{{}^0N(t) = m\} \to e^{-\lambda}\frac{\lambda^m}{m!} \qquad (n \to \infty)$$

for every nonnegative integer m.

We prove these propositions in turn.

A. Single Vertex Isolation

We begin by considering the progress of a single vertex, say X_i, toward isolation. This is the key to the proof and the results of the analysis will be in repeated use in subsequent stages.

Recall that the points $X_1, \ldots, X_n$ are generated by independent sampling from the uniform distribution in the unit circle in the Euclidean plane. The unit circle hence comprises the *sensor field*. In the graph $\mathcal{G}_{n,r}$, vertices adjacent to X_i must lie in the region defined by the intersection of the unit circle with the circle of radius r centered at X_i. We call this the *region of visibility* of vertex X_i. By symmetry it is clear that the area $A = A(X_i)$ of the region of visibility depends only on the distance of X_i from the origin (see Fig. 1).

Given X_i, the conditional probability that any other vertex X_j is adjacent to X_i is given by $a(X_i) = A(X_i)/\pi$ so that the number of vertices adjacent to X_i corresponds to the number of successes in $n-1$ tosses of a bent coin with success probability $a(X_i)$. As each vertex progresses to failure independently with common distribution function $F(t) = F_{c_n}(t)$ for the time to failure, given X_i the conditional probability that vertex X_i is isolated by time t in $\mathcal{G}_{n,r}$ satisfies

$$\begin{aligned}&\mathbf{P}\left({}^0L_i(t) \,|\, X_i\right)\\ &\quad= \sum_{k=0}^{n-1}\binom{n-1}{k} a(X_i)^k\,(1-a(X_i))^{n-1-k}\,F(t)^k\\ &\quad= [a(X_i)F(t) + (1-a(X_i))]^{n-1}\\ &\quad= (1-a(X_i)G(t))^{n-1}\end{aligned}$$

where, as before, $G(t) = 1 - F(t)$ is the right tail of the lifetime distribution. Take expectation with respect to X_i to get rid of the conditioning and obtain

$${}^0P(t) = \mathbf{E}\{\mathbf{P}({}^0L_i(t) \,|\, X_i)\} = \mathbf{E}\{(1-a(X_i)G(t))^{n-1}\}. \tag{5}$$

Henceforth we will suppose that $r = r_n, c = c_n$, and $t = t_n$ satisfy the theorem conditions (2″).

Some preliminary spadework helps put subsequent expressions into an analytically amenable framework. Observe that $A(X_i) \le \pi r^2$ whence $a(X_i) \le r^2$ with equality in the interior of the unit circle. As $\log(1-x) = -x + \mathcal{O}(x^2)$ and $e^x = 1 + \mathcal{O}(x)$ as $x \to 0$, an easy application of Lemma 1 now shows that

$$\begin{aligned}&(1-a(X_i)G(t))^{n-1}\\ &\quad= e^{n\log(1-a(X_i)G(t))}(1-a(X_i)G(t))^{-1}\\ &\quad= e^{-na(X_i)G(t)+\mathcal{O}(nr^4G^2(t))}[1+\mathcal{O}(r^2G(t))]\\ &\quad= e^{-na(X_i)G(t)}\left[1+\mathcal{O}\left(\frac{\log^2 n}{n}\right)\right]\end{aligned}$$

where the order bound is uniform in X_i. It follows:

$${}^0P(t) = \left[1+\mathcal{O}\left(\frac{\log^2 n}{n}\right)\right]\mathbf{E}\left(e^{-na(X_i)G(t)}\right) \qquad (n \to \infty) \tag{6}$$

and it suffices hence to evaluate

$$I(n) \triangleq \mathbf{E}\left(e^{-na(X_i)G(t)}\right) = \frac{1}{\pi}\int e^{-na(x_i)G(t)}\,dx_i \tag{6′}$$

where the integral ranges over all points in the unit disc $\mathbb{D}_i(1;0) = \{x_i : |x_i| \le 1\}$.[2]

The observation that $A(X_i)$, hence also $a(X_i)$, depends only on the distance $|X_i|$ of vertex X_i from the origin helps further simplify the expression. The distance $|X_i|$ of vertex X_i from the field center is a random variable with distribution function $\mathbf{P}\{|X_i| \le \rho\} = \pi\rho^2/\pi = \rho^2$ for $0 \le \rho \le 1$. It follows that $|X_i|$ has density 2ρ $(0 \le \rho \le 1)$. In a slight abuse of notation, write $a(X_i) = a_{|X_i|}$ to emphasize the dependence of a on the length of X_i alone. We hence have

$$I(n) = \mathbf{E}\left(e^{-na_{|X_i|}G(t)}\right) = \int_0^1 2\rho e^{-na_\rho G(t)}\,d\rho.$$

It is expedient to partition the range of the integral and write $I(n) = I_{\text{interior}} + I_{\text{boundary}}$ where I_{interior} is the contribution to the integral from the interior of the unit circle $0 \le \rho \le 1 - r$

[2]The words disc and circle are used interchangeably for our purposes.

and I_{boundary} is the contribution to the integral from the annulus $1-r<\rho\le 1$ at the boundary. We evaluate these contributions in turn.

The interior contribution. When $0\le\rho\le 1-r$, the point X_i is in the interior of the unit circle and the circle of radius r centered at X_i is contained wholly within the sensor field as illustrated in Fig. 1(a). It follows that $a_\rho=\pi r^2/\pi=r^2$ hence

$$I_{\text{interior}}=\int_0^{1-r}2\rho e^{-na_\rho G(t)}\,d\rho=e^{-nr^2G(t)}(1-r)^2 =e^{-nr^2G(t)}\left[1+\mathcal{O}\left(\frac{\log n}{\sqrt{n}}\right)\right]$$

asymptotically as $n\to\infty$. And, *a fortiori*, we have established the following estimate.

Assertion 1: The interior contribution satisfies the asymptotic relation $I_{\text{interior}}\sim\lambda/n$ as $n\to\infty$.

The boundary contribution. When $1-r<\rho\le 1$, the point X_i lies in an asymptotically vanishing annulus of width r at the boundary of the unit circle. The region of visibility is now a lens as shown in the shaded region in Fig. 1(b) and it is clear that a_ρ decreases monotonically from r^2 to a value close to $r^2/2$ as ρ increases from $1-r$ to 1. We cannot simply ignore losses at the boundary, tempting as it is to do so, as an isolated vertex on the boundary will result in a significant sensory lacuna in the sensor field, the size of the lacuna being at least half that of a lacuna at an isolated vertex in the interior.

The situation at the boundary is extremely delicate. On the face of it, the probability that a vertex lands in the boundary is small so that other things being equal the boundary should contribute very little to the probability of isolation. However, in the boundary annulus the area of a vertex's region of visibility is about one-half of its area in the interior, in consequence fewer vertices are adjacent to it, and hence the chances of isolation increase as isolation now requires the extinction of fewer vertices than in the interior. The contribution to the probability of isolation from the boundary is dynamically balanced between these two opposing effects, the critical factor being the rate of decrease of the radius of communication $r=r_n$ with n. It transpires that, for the given rate $r_n=\mathfrak{o}(\frac{\log n}{\sqrt{n}})$ (but no larger), the contribution of the boundary is asymptotically subdominant vis à vis that of the interior.

Assertion 2: The boundary contribution satisfies the asymptotic relation $I_{\text{boundary}}=\mathfrak{o}(n^{-1})$ as $n\to\infty$.

We defer the proof of the assertion to Appendix A in an effort to keep focused on the dominant behaviors.[3]

In accordance with naive expectation, the boundary contributes an asymptotically negligible amount to the isolation probability for the given maximal rate of variation of r (though the conclusion is false for rates of variation larger than prescribed). Combining the interior and boundary estimates for the integral, we obtain

$$I(n)=I_{\text{interior}}+I_{\text{boundary}}=\frac{\lambda}{n}(1+\mathfrak{o}(1))+\mathfrak{o}(\frac{1}{n}).$$

From (6), (6′) it follows that, as advertised, *the probability that any given vertex is isolated by time t in $\mathcal{G}_{n,r}$ satisfies* ${}^0P(t)\sim I(n)\sim\frac{\lambda}{n}$ *as* $n\to\infty$. This concludes the proof of Proposition 1.

Observe, in particular, that the expected number of isolated vertices at time $t=t_n$ in $\mathcal{G}_{n,r}$ satisfies $\mathbf{E}({}^0N(t))\to\lambda$ as $n\to\infty$. We now proceed to refine this crude estimate.

B. Conjunctions of Vertex Isolations

The new features that are encountered in moving from one vertex to several vertices are statistical dependencies that arise due to overlaps of visibility regions as well as slightly more complicated boundary interactions. We will keep the burgeoning complexity under bounds by reducing considerations of dependencies that accrue for groups of vertices to repeated considerations of vertex pairs.

Let us pause here to introduce some new notation. As before, write $\mathbb{D}(z;x)$ for the closed disc of radius z centered at the point x in the plane. Let $\mathbb{S}=\mathbb{D}(1;0)$ be the unit disc centered at the origin. This is, of course, the sensor field. We also write $\mathbb{V}(x)=\mathbb{D}(r;x)\cap\mathbb{S}$ for the region of visibility of a sensor located at point x. For brevity, we say simply that $\mathbb{V}(x)$ is the region of visibility of the point x. We also define the *overlap region* of a sensor located at point x by $\mathbb{O}(x)=\mathbb{D}(2r;x)\cap\mathbb{S}$. The motivation arises from the observation that if $x_2\in\mathbb{O}(x_1)$ then $\mathbb{V}(x_1)\cap\mathbb{V}(x_2)\neq\emptyset$ and the regions of visibility of the two points overlap. Overlap regions will be important in the characterization of dependencies. Finally, in a slight but hopefully natural modification of an earlier notation, write $A_k(x_1,\dots,x_k)=\int_{\mathbb{V}(x_1)\cup\dots\cup\mathbb{V}(x_k)}dx$ for the area of the conjoined visibility region $\mathbb{V}(x_1)\cup\cdots\cup\mathbb{V}(x_k)$ of the points $x_1,\dots,x_k$. Specializing to $k=1$ and 2, $A_1(x)$ is the area of the visibility region of point x (replacing the earlier notations $A(x)$ and $A_{|x|}$) and $A_2(x_1,x_2)$ is the area of $\mathbb{V}(x_1)\cup\mathbb{V}(x_2)$. Finally write $a_k(x_1,\dots,x_k)=\frac{1}{\pi}A_k(x_1,\dots,x_k)$ for the probability that a randomly selected point in the unit disc $\mathbb{S}$ falls in the region of visibility of at least one of the k points $x_1,\dots,x_k$. In particular, $a_1(x)$ is the probability that a randomly selected point falls in $\mathbb{V}(x)$ (replacing the earlier notations $a(x)$ and $a_{|x|}$) and $a_2(x_1,x_2)$ is the probability that a randomly selected point falls in $\mathbb{V}(x_1)\cup\mathbb{V}(x_2)$.

Fix any positive integer $k\ge 2$ and let $X_{i_1},\dots,X_{i_k}$ be any collection of k distinct vertices. We now proceed to estimate the probability of the event ${}^0L_{i_1,\dots,i_k}(t)={}^0L_{i_1}(t)\cap\cdots\cap{}^0L_{i_k}(t)$ that each of the k vertices $X_{i_1},\dots,X_{i_k}$ is isolated by time t. By symmetry, $\mathbf{P}({}^0L_{i_1,\dots,i_k}(t))=\mathbf{P}({}^0L_{1,\dots,k}(t))$ and we may without loss of generality focus on vertices X_1 through X_k.

Given the random k-tuple of points $(X_1,\dots,X_k)$, the conditional probability that vertices X_1 through X_k are isolated is a random variable $\mathbf{P}({}^0L_{1,\dots,k}(t)\,|\,X_1,\dots,X_k)$ that takes the value $\mathbf{P}({}^0L_{1,\dots,k}(t)\,|\,X_1=x_1,\dots,X_k=x_k)$ at sample points in the space characterized by the joint occurrence of the events

[3]It should be remarked that the calculations of the ultimately subdominant boundary effects cannot be escaped. Indeed, in three and more dimensions the contribution from the boundary is dominant over the interior; it is only in one and two dimensions that the boundary has negligible effect. Proving this unfortunately requires substantial effort and the bulk of our proof is devoted to showing the subdominance of the boundary in the 2-D setting.

$\{X_1 = x_1\}, \ldots, \{X_k = x_k\}$. As $X_1, \ldots, X_n$ are drawn by independent sampling from the uniform distribution on the unit disc we have

$$\mathbf{P}\left({}^0L_{1,\ldots,k}(t)\right) = \mathbf{E}\left[\mathbf{P}\left({}^0L_{1,\ldots,k}(t) \mid X_1, \ldots, X_k\right)\right]$$

$$= \frac{1}{\pi^k}\int\cdots\int_{\mathbb{S}^k} \mathbf{P}({}^0L_{1,\ldots,k}(t) \,|\, X_1 = x_1, \ldots, X_k = x_k)\, dx_k \ldots dx_1. \quad (7)$$

It will again be expedient to partition the range of the integral. But first, one more definition.

The overlap graph. Every choice of points $x_1, \ldots, x_k$ in $\mathbb{S}$ induces a graph $\mathcal{H}_k(x_1, \ldots, x_k)$ on the set of vertices $\{1, \ldots, k\}$ whose edges are all vertex pairs (i, j) for which $|x_i - x_j| \leq 2r$, that is to say, $\mathbb{V}(x_i) \cap \mathbb{V}(x_j) \neq \emptyset$. We call $\mathcal{H}_k(x_1, \ldots, x_k)$ an *overlap graph*. Each overlap graph $\mathcal{H}_k(x_1, \ldots, x_k)$ may be partitioned into $\gamma = \gamma(x_1, \ldots, x_k)$ *components* $\{\mathcal{H}_k(1), \ldots, \mathcal{H}_k(\gamma)\}$ where $1 \leq \gamma \leq k$ and each component $\mathcal{H}_k(l)$ is a connected sub-graph with no out-going edges. (More formally, if $\mathcal{H}_k(l)$ and $\mathcal{H}_k(m)$ are two distinct components then $\mathcal{H}_k$ exhibits no edges (i, j) where i is a vertex of $\mathcal{H}_k(l)$ and j is a vertex of $\mathcal{H}_k(m)$.)

Now any graph $\mathcal{F}$ on the vertices $\{1, \ldots, k\}$ induces an equivalence class $\mathbb{C}(\mathcal{F})$ of k-tuples of points $(x_1, \ldots, x_k)$ in $\mathbb{S}^k$ whose overlap graph $\mathcal{H}_k(x_1, \ldots, x_k)$ coincides with $\mathcal{F}$. As each k-tuple of points $(x_1, \ldots, x_k)$ in $\mathbb{S}^k$ belongs to one and only one equivalence class $\mathbb{C}(\mathcal{F})$, as $\mathcal{F}$ varies over all graphs on k vertices the sets $\mathbb{C}(\mathcal{F})$ partition $\mathbb{S}^k$ into $2^{\binom{k}{2}}$ nonoverlapping regions. We may hence partition the integral on the right-hand side of (7) and write

$$\mathbf{P}({}^0L_{1,\ldots,k}(t)) = \sum_{\mathcal{F}} \mathbf{E}\left[1_{\mathbb{C}(\mathcal{F})}(X_1, \ldots, X_k) \times \mathbf{P}\left({}^0L_{1,\ldots,k}(t) \,|\, X_1, \ldots, X_k\right)\right] \quad (8)$$

where the sum ranges over all $2^{\binom{k}{2}}$ graphs $\mathcal{F}$ on k vertices and we use the generic indicator function notation

$$1_{\mathcal{A}}(\zeta) = \begin{cases} 1, & \text{if } \zeta \in \mathcal{A} \\ 0, & \text{if } \zeta \notin \mathcal{A}. \end{cases}$$

Of particular interest is the graph $\mathcal{F}_*$ obtained when the vertices $\{1, \ldots, k\}$ form an independent set, that is to say, the graph has no edges. Clearly $\mathcal{F}_*$ is the unique graph with $\gamma = k$ components, each component consisting of course of a singleton vertex. The corresponding equivalence class $\mathbb{C}(\mathcal{F}_*)$ consists of k-tuples of points $(x_1, \ldots, x_k)$ where the x_i have mutually nonoverlapping regions of visibility, that is to say, $\mathbb{V}(x_i) \cap \mathbb{V}(x_j) = \emptyset$ if $i \neq j$. The remaining graphs $\mathcal{F} \neq \mathcal{F}_*$ contain $1 \leq \gamma \leq k-1$ components and correspond to overlap graphs induced by points $x_1, \ldots, x_k$ for which at least two regions of visibility overlap. We separate these cases for consideration and write

$$J_{\text{nonoverlap}} = \mathbf{E}\left[1_{\mathbb{C}(\mathcal{F}_*)}(X_1, \ldots, X_k) \times \mathbf{P}({}^0L_{1,\ldots,k}(t) \,|\, X_1, \ldots, X_k)\right]$$

$$J_{\text{overlap}} = \sum_{\mathcal{F} \neq \mathcal{F}_*} \mathbf{E}\left[1_{\mathbb{C}(\mathcal{F})}(X_1, \ldots, X_k) \times \mathbf{P}({}^0L_{1,\ldots,k}(t) \,|\, X_1, \ldots, X_k)\right]. \quad (9)$$

Then $\mathbf{P}({}^0L_{1,\ldots,k}(t)) = J_{\text{nonoverlap}} + J_{\text{overlap}}$ and we proceed to evaluate these contributions in turn.

Nonoverlapping regions of visibility; independent sets and the overlap graph $\mathcal{F}_*$. The set of points $(x_1, \ldots, x_k)$ forming the equivalence class $\mathbb{C}(\mathcal{F}_*)$ may be systematically specified by the following recursive procedure.

BASE: The point x_1 is allowed to range over all points in the unit disc $\mathbb{S}$.

RECURRENCE: As j ranges from 2 to k, for every selection of $x_1, \ldots, x_{j-1}$, the point x_j is allowed to range over the set of points $\mathbb{S} \setminus \bigcup_{i=1}^{j-1} \mathbb{O}(x_i)$ consisting of the unit disc with the overlap regions of the points $x_1, \ldots, x_{j-1}$ excised.

It is clear from the recursive construction that the points $x_1, \ldots, x_k$ specified thus have nonoverlapping regions of visibility and, furthermore, a little thought shows that indeed this process covers all the points in $\mathbb{C}(\mathcal{F}_*)$. We are now ready for the main estimate.

Assertion 3: The contribution from graphs with nonoverlapping regions of visibility satisfies the asymptotic relation $J_{\text{nonoverlap}} \sim \lambda^k/n^k$ as $n \to \infty$.

Proof: Suppose $(x_1, \ldots, x_k) \in \mathbb{C}(\mathcal{F}_*)$ so that the x_i have mutually nonoverlapping regions of visibility. Then $a_k(x_b 1, \ldots, x_k) = a_1(x_1) + \cdots + a_1(x_k)$ where each $\mathrm{b}a_1(x_i) \leq r^2$ (with equality if, and only if, x_i is an interior point). Following the line of argument leading up to (5) and (6) we then obtain

$$\begin{aligned}
&\mathbf{P}\left({}^0L_{1,\ldots,k}(t) \,|\, X_1 = x_1, \ldots, X_k = x_k\right) \\
&\quad = (1 - a_k(x_1, \ldots, x_k)G(t))^{n-k} \\
&\quad = \left[1 + \mathcal{O}\left(\frac{\log^2 n}{n}\right)\right] e^{-na_k(x_1,\ldots,x_k)G(t)} \\
&\quad = \left[1 + \mathcal{O}\left(\frac{\log^2 n}{n}\right)\right] \prod_{j=1}^{k} e^{-na_1(x_j)G(t)}
\end{aligned}$$

where the order term is uniform over all choices of $x_1, \ldots, x_k$. By systematically conditioning on X_1 first, then X_2, and so on, and finally conditioning on X_k, we obtain

$$\begin{aligned}
J_{\text{nonoverlap}} &= \left[1 + \mathcal{O}\left(\frac{\log^2 n}{n}\right)\right] \\
&\quad \times \mathbf{E}\left(1_{\mathbb{C}(\mathcal{F}_*)}(X_1, \ldots, X_k) \prod_{j=1}^{k} e^{-na_1(X_j)G(t)}\right) \\
&= \left[1 + \mathcal{O}\left(\frac{\log^2 n}{n}\right)\right] \frac{1}{\pi}\int_{\mathbb{S}} dx_1 e^{-na_1(x_1)G(t)} \\
&\quad \times \frac{1}{\pi}\int_{\mathbb{S}\setminus\mathbb{O}(x_1)} dx_2 e^{-na_1(x_2)G(t)} \\
&\quad \cdots \frac{1}{\pi}\int_{\mathbb{S}\setminus\bigcup_{i=1}^{k-1}\mathbb{O}(x_i)} dx_k e^{-na_1(x_k)G(t)}.
\end{aligned}$$

A typical nested integral on the right-hand side is of the form

$$\frac{1}{\pi}\int_{\mathbb{S}\setminus\bigcup_{i=1}^{j-1}\mathbb{O}(x_i)} dx_j e^{-na_1(x_j)G(t)} = \frac{1}{\pi}\int_{\mathbb{S}} dx_j e^{-na_1(x_j)G(t)} - \frac{1}{\pi}\int_{\bigcup_{i=1}^{j-1}\mathbb{O}(x_i)} dx_j e^{-na_1(x_j)G(t)}.$$

The first integral on the right is, up to a multiplicative factor of $1+\mathfrak{o}(1)$, just the probability that vertex X_j is isolated by time t in $\mathcal{G}_{n,r}$ (see (6), (6′)) hence

$$\frac{1}{\pi}\int_{\mathbb{S}} dx_j e^{-na_1(x_j)G(t)} \sim {}^0P(t) \sim \frac{\lambda}{n} \qquad (n\to\infty)$$

from our considerations for a single vertex. As for the second of the two integrals on the right, it is clear that $a_1(x_j)$ achieves its minimum value when x_j lies on the perimeter of the unit disc and this smallest value is close to $r^2/2$; indeed, in Appendix A we show that $a_1(x_j)\geq \frac{1}{2}r^2-\frac{1}{\pi}r^3$ for large enough n (see (18)), and accordingly we may bound

$$\begin{aligned}
&\frac{1}{\pi}\int_{\bigcup_{i=1}^{j-1}\mathbb{O}(x_i)} dx_j e^{-na_1(x_j)G(t)}\\
&\quad\leq e^{-\frac{1}{2}nn^2G(t)+\frac{1}{\pi}nr^3G(t)}\left(\frac{1}{\pi}\int_{\bigcup_{i=1}^{j-1}\mathbb{O}(x_i)} dx_j\right)\\
&\quad\leq (j-1)4r^2e^{-\frac{1}{2}nr^2G(t)+\frac{1}{\pi}nr^3G(t)}\\
&\quad= (j-1)4r^2\sqrt{\frac{\lambda}{n}}\,(1+\mathfrak{o}(1))(1+\mathcal{O}(r\log n))\\
&\quad= \mathcal{O}\left(\frac{r^2}{\sqrt{n}}\right)=\mathfrak{o}\left(\frac{\log^2 n}{n^{3/2}}\right)
\end{aligned}$$

where the order term is uniform with respect to the x_i. Consequently

$$\begin{aligned}
&\frac{1}{\pi}\int_{\mathbb{S}\setminus\bigcup_{i=1}^{j-1}\mathbb{O}(x_i)} dx_j e^{-na_1(x_j)G(t)}\\
&\qquad\qquad=\frac{\lambda}{n}\left[1+\mathfrak{o}(1)+\mathfrak{o}\left(\frac{\log^2 n}{\sqrt{n}}\right)\right] \qquad (10)
\end{aligned}$$

for each j and we obtain the estimate

$$\begin{aligned}
J_{\text{nonoverlap}}=\frac{\lambda^k}{k!}\Bigg[1+\mathfrak{o}(1)+\mathfrak{o}\left(\frac{\log^2 n}{\sqrt{n}}\right)\\
+\mathcal{O}\left(\frac{\log^2 n}{n}\right)\Bigg]\sim\frac{\lambda^k}{n^k} \qquad (11)
\end{aligned}$$

asymptotically as $n\to\infty$.

Overlapping regions of visibility preliminaries; connected overlap graphs: We may systematically group graphs $\mathcal{F}$ on k vertices according to 1) the number of components $\gamma=\gamma(\mathcal{F})$ of the graph and 2) the sizes of the components $k_1,\ldots,k_\gamma$. Define

$$\begin{aligned}
J_{k_1,\ldots,k_\gamma}\triangleq\sum_{\mathcal{F}_{k_1,\ldots,k_\gamma}}\mathbf{E}\Big[1_{\mathbb{C}(\mathcal{F}_{k_1,\ldots,k_\gamma})}(X_1,\ldots,X_k)\\
\times\mathbf{P}\left({}^0L_{1,\ldots,k}(t)\mid X_1,\ldots,X_k\right)\Big] \qquad (12)
\end{aligned}$$

where, in an obvious notation, the sum on the right ranges over all graphs $\mathcal{F}_{k_1,\ldots,k_\gamma}$ with γ components of sizes $k_1,\ldots,k_\gamma$.[4] As graphs in the family $\{\mathcal{F}:\mathcal{F}\neq\mathcal{F}_*\}$ have a number of components varying between $1\leq\gamma\leq k-1$ we accordingly obtain

$$J_{\text{overlap}}=\sum_{\gamma=1}^{k-1}\sum_{\substack{k_1\geq\cdots\geq k_\gamma\geq 1\\ k_1+\cdots+k_\gamma=k}} J_{k_1,\ldots,k_\gamma}. \qquad (12')$$

Most of the effort in the proof of the MAIN THEOREM goes into showing that the contributions from the terms $J_{k_1,\ldots,k_\gamma}$ are ultimately negligible in the range under consideration.

Assertion 4: The asymptotic order relation $J_{k_1,\ldots,k_\gamma}=\mathfrak{o}(n^{-k})$ holds for every fixed choice of $k_1,\ldots,k_\gamma$ and consequently the contribution from graphs with overlapping regions of visibility satisfies $J_{\text{overlap}}=\mathfrak{o}(n^{-k})$ as $n\to\infty$.

Again, as in the case of Assertion 2, we defer the technically involved proof of these sub-dominant effects till Appendix B to allow us to focus on the dominant behaviors.

Joint isolation probability. Assertions 3 and 4 complete our evaluation of the system of equations (9). Returning finally to (8) we obtain

$$\begin{aligned}
\mathbf{P}\left({}^0L_{1,\ldots,k}(t)\right)&=J_{\text{nonoverlap}}+J_{\text{overlap}}\\
&=\frac{\lambda^k}{n^k}(1+\mathfrak{o}(1))+\mathfrak{o}(n^{-k})\sim\frac{\lambda^k}{n^k}.
\end{aligned}$$

It follows that, as claimed, as $n\to\infty$, *the asymptotic relation* $\mathbf{P}({}^0L_{i_1,\ldots,i_k}(t))\sim\frac{\lambda^k}{n^k}$ *holds for any fixed positive integer* k *and any collection of* k *distinct indices* $i_1,\ldots,i_k$. Recall that our analysis for a single vertex revealed that $\mathbf{P}({}^0L_i(t))={}^0P(t)\sim\frac{\lambda}{n}$. Thus, for any group of k vertices we have shown that $\mathbf{P}({}^0L_{i_1}(t)\cap\cdots\cap{}^0L_{i_k}(t))\sim[{}^0P(t)]^k$ and we may paraphrase this succinctly, if somewhat imprecisely, by saying that the events ${}^0L_i(t)$ are weakly asymptotically independent. This completes the proof of Proposition 2.

C. A Poisson Sieve

The stage is set for an application of Bonferroni's inequalities (Lemma 2). Let $S_k(n)$ denote the sum of all the probabilities of k-fold conjunctions of the events ${}^0L_i(t)$ $(1\leq i\leq n)$. As $n\to\infty$ we obtain

$$\begin{aligned}
S_k(n)&=\sum_{1\leq i_1<\cdots<i_k\leq n}\mathbf{P}\left({}^0L_{i_1}(t)\cap\cdots\cap{}^0L_{i_k}(t)\right)\\
&=\binom{n}{k}\mathbf{P}\left({}^0L_{1,\ldots,k}(t)\right)\sim\binom{n}{k}\frac{\lambda^k}{n^k}.
\end{aligned}$$

Now $\binom{n}{k}=\frac{1}{k!}n(n-1)\ldots(n-k+1)=\frac{n^k}{k!}[1+\mathcal{O}(\frac{1}{n})]\sim\frac{n^k}{k!}$ where, of course, k is fixed and n tends to infinity. It follows that, for every positive integer k, $S_k(n)\to\frac{\lambda^k}{k!}$ as $n\to\infty$. Hence, for every fixed K

$$\begin{aligned}
&\sum_{k=0}^{K}(-1)^k\binom{m+k}{m}S_{m+k}(n)\\
&\qquad\to\sum_{k=0}^{K}\frac{(-1)^k\lambda^{m+k}}{(m+k)!}\,\frac{(m+k)!}{m!k!}=\frac{\lambda^m}{m!}\sum_{k=0}^{K}\frac{(-\lambda)^k}{k!}
\end{aligned}$$

[4] In this new notation the graph $\mathcal{F}_*$ may be identified with the unique graph $\mathcal{F}_{1,\ldots,1}$ but we will not be pedagogically fussy here.

as $n \to \infty$. We recognize the truncated Taylor series for $e^{-\lambda}$ on the right-hand side. As the exponential series $e^x = \sum_{k=0}^{\infty} x^k/k!$ converges absolutely (and uniformly over every closed and bounded interval) it follows that for every $\epsilon > 0$ we can select $K = K(\epsilon)$ so that

$$\left| \sum_{k=0}^{K} \frac{(-\lambda)^k}{k!} - e^{-\lambda} \right| < \epsilon.$$

Let m be any nonnegative integer. Then the event $\{{}^0N(t) = m\}$ that there are exactly m isolated vertices at time t in the graph $\mathcal{G}_{n,r}$ occurs if, and only if, precisely m of the events $\{{}^0L_i(t), 1 \le i \le n\}$ occur. By Lemma 2, for every $\epsilon > 0$ we may select a sufficiently large value of K so that

$$\begin{aligned}(e^{-\lambda} - \epsilon)\frac{\lambda^m}{m!} &< \sum_{k=0}^{2K-1} (-1)^k \binom{m+k}{m} S_{m+k}(n) \\ &\le \mathbf{P}\left\{{}^0N(t) = m\right\} \\ &\le \sum_{k=0}^{2K} (-1)^k \binom{m+k}{m} S_{m+k}(n) \\ &< (e^{-\lambda} + \epsilon)\frac{\lambda^m}{m!}\end{aligned}$$

with the book-end inequalities on either side holding for all sufficiently large n. As the tiny ϵ is arbitrary, it follows that $\mathbf{P}\{{}^0N(t) = m\} \to e^{-\lambda}\lambda^m/m!$ as $n \to \infty$, as advertised. This completes the proof of Proposition 3 and hence of the MAIN THEOREM for the case of isolated vertices $\ell = 0$ in the graph $\mathcal{G}_{n,r}$. □

D. Mopping Up

The proofs of the general result and the corollaries require only small adaptations to the framework of the proof for isolated vertices.

PROOF OF THE MAIN THEOREM: Recall that the disc $\mathbb{D}_i(\ell)$ is isolated at time t in $\mathcal{G}_{n,r}$ if the annulus $\mathbb{D}_i(\ell, \ell + r)$ contains no live vertices at time t. Adapt the earlier notation and write $A(X_i)$ for the area of the intersection of $\mathbb{D}_i(\ell, \ell + r)$ with the unit disc $\mathbb{S}$. Then $a(X_i) = A(X_i)/\pi$ is the probability that a random vertex will lie in $\mathbb{D}_i(\ell, \ell + r) \cap \mathbb{S}$. Arguing as before, conditioned on X_i the probability that $\mathbb{D}_i(\ell)$ is isolated at time t in $\mathcal{G}_{n,r}$ is then $(1 - a(X_i)G(t))^{n-1}$. Taking expectation gives us the unconditional probability of isolation of the disc of radius ℓ centered at the ith vertex

$${}^{\ell}P(t) = \mathbf{E}\{(1 - a(X_i)G(t))^{n-1}\} \tag{5'}$$

which generalizes the corresponding expression (5) for isolated vertices.

It is clear, as before, that $a(X_i)$ depends only on $|X_i|$, the distance of X_i from the origin. If X_i lies in the interior of the unit disc with $|X_i| \le 1 - \ell - r$ then $a(X_i) = (\ell + r)^2 - \ell^2 = 2\ell r + r^2 \triangleq R^2$ with $a(X_i)$ decreasing monotonically thereafter to a value close to $R^2/2$ as $|X_i|$ increases from $1 - \ell - r$ to 1; see Fig. 2. Redefine the interior to mean the region $|X_i| \le 1 - \ell - r$. The interior contribution to the expectation integral (5′) is then asymptotic to $e^{-nR^2G(t)}$. Arguing as for an isolated vertex, the contribution of the boundary to ${}^{\ell}P(t)$ is subdominant so that ${}^{\ell}P(t) \sim e^{-nR^2G(t)} \sim \lambda/n$ under the conditions of the MAIN THEOREM.

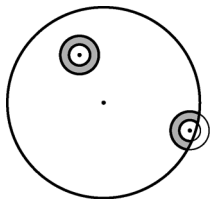

Fig. 2. Visibility annuli.

The rest of the proof proceeds exactly as before with the systematic replacement of references to r in the proof for isolated vertices by $R = \sqrt{2\ell r + r^2}$. The steps in the proof remain unaltered with the geometry only slightly messier as annuli replace discs of visibility. We eschew the unedifying details. □

The corollaries all follow quickly as indicated in Section IV with only Corollary 7 needing further comment.

Proof of Corollary 7: Recall that there is a lacuna of radius ℓ centered at vertex X_i at time t if there are no live vertices in (1) the annulus $\mathbb{D}_i(\ell, \ell + s)$, and (2) at least one of the disc $\mathbb{D}_i(\ell)$ and the annulus $\mathbb{D}_i(\ell, \ell + c)$. Temporarily write $Q_n = Q_n(\ell, s, c, t)$ for the probability that there is a lacuna of radius ℓ centered at a network vertex at time t. There are two cases possible depending on whether $s > c$ or $s \le c$. We consider these in turn.

Suppose $s > c$. Clearly, if there are no live vertices in $\mathbb{D}_i(\ell, \ell + s)$ then there will certainly be no live vertices in $\mathbb{D}_i(\ell, \ell + c)$ so that condition (2) follows trivially if condition (1) holds. Consequently, there is a lacuna of radius ℓ centered at vertex X_i at time t if, and only if, at time t there are no live vertices in $\mathbb{D}_i(\ell, \ell + s)$, or, equivalently, the disc $\mathbb{D}_i(\ell)$ is isolated in the graph $\mathcal{G}_{n,s}$. Arguing as in the MAIN THEOREM for an isolated disc, it follows that

$$Q_n \sim e^{-n[(\ell+s)^2 - \ell^2]G(t)}. \tag{13}$$

when $s > c$.

Now consider the case $s \le c$. There are two mutually exclusive cases depending on whether there are any live vertices in the disc $\mathbb{D}_i(\ell)$.

1) Conditioned on the event that there are no live vertices in $\mathbb{D}_i(\ell)$ at time t, there will be a lacuna of radius ℓ centered at X_i at time t if, and only if, there are no live vertices in $\mathbb{D}_i(\ell, \ell + s)$ at that time. The probability that there are no live vertices in both $\mathbb{D}_i(\ell)$ and $\mathbb{D}_i(\ell, \ell + s)$ is equal to the probability that vertex X_i is extinguished as well as isolated in $\mathcal{G}_{n,\ell+s}$ and the line of argument leading to the MAIN THEOREM shows that this is asymptotic to

$$(1 - G(t))e^{-n(\ell+s)^2 G(t)} \tag{14}$$

as the extinction of the vertex X_i is independent of the extinction of other vertices.

2) Conditioned on the event that there exist live vertices in $\mathbb{D}_i(\ell)$ at time t, there will be a lacuna of radius ℓ centered at X_i at time t if, and only if, there are no live vertices in $\mathbb{D}_i(\ell, \ell +$

c) (as this event will also imply that there are no live vertices in $\mathbb{D}_i(\ell, \ell+s)$ when $s \leq c$), or, equivalently, disc $\mathbb{D}_i(\ell)$ is isolated in $\mathcal{G}_{n,c}$. Arguing as in (14), the probability that there are live vertices in the disc $\mathbb{D}_i(\ell)$ at time t is asymptotic to $1-(1-G(t))e^{-n\ell^2 G(t)}$ and, likewise, following the line of the MAIN THEOREM, the probability that $\mathbb{D}_i(\ell)$ is isolated in $\mathcal{G}_{n,c}$ at time t is asymptotic to $e^{-n[(\ell+c)^2-\ell^2]G(t)}$. As vertex extinctions are independent, it follows that the probability that, at time t, the disc $\mathbb{D}_i(\ell)$ contains live vertices but is isolated in $\mathcal{G}_{n,c}$ is asymptotic to

$$e^{-n[(\ell+c)^2-\ell^2]G(t)}\left\{1-(1-G(t))\,e^{-n\ell^2 G(t)}\right\} = e^{-n[(\ell+c)^2-\ell^2]G(t)} - (1-G(t))\,e^{-n(\ell+c)^2 G(t)}. \quad (15)$$

Combining the asymptotic estimates (14) and (15), we obtain

$$Q_n \sim e^{-n[(\ell+c)^2-\ell^2]G(t)} + (1-G(t)) \times \left\{e^{-n(\ell+s)^2 G(t)} - e^{-n(\ell+c)^2 G(t)}\right\} \quad (16)$$

when $s \leq c$.

The right-hand sides of (13) and (16) may be combined into the single expression $P_n = P_n(\ell, s, c, t)$ given by (3). Accordingly, we have shown that the probability that there is a lacuna of radius ℓ at any given network vertex at time t is given asymptotically by $Q_n \sim P_n \sim \lambda/n$ under the conditions of the corollary. The rest of the proof follows the steps of the proof for single vertex isolation. Following that line of argument, the probability that there are lacunae of radius ℓ at any k given network vertices at time t is asymptotic to $\lambda^k/k!$ and inclusion–exclusion completes the proof as before. □

VI. CONCLUDING REMARKS

The phase transitions that are so characteristic of random graph phenomena make their appearance in this setting in the time to emergence of sensory lacunae. The Poisson laws that are the content of our MAIN THEOREM provide a detailed picture of the situation at the critical time; these results provide explicit and fundamental tradeoffs between transmission power, vertex density, and network lifetime and suggest, as we saw in the examples of Section III, how principled choices can be made to improve the lifetime of the network.

Several other questions are suggested in this framework. For instance, one may wish to track how network connectivity evolves as vertices are extinguished. In particular, one may wish to characterize when connectivity among vertex *survivors* first breaks down. In a concurrent paper we demonstrate that survivor connectivity also exhibits a phase transition at a critical time [11].

The conditions under which our theorem operates are of course highly sanitised and several points of departure toward more complicated (and perhaps realistic) models are suggested. We discuss a few of these.

From circular to noncircular and irregular regions of deployment: A consideration of the proof of the MAIN THEOREM shows that most of the effort was expended in showing that boundary and overlap effects are ultimately negligible in a certain domain. It should be clear from the analysis that the result, while presented for a circular sensor field, should carry through to other shapes as well; roughly speaking, all that is required is that the perimeter does not dominate the interior. Thus, "fat" or "blobby" shapes are in; "thin" or "squiggly" shapes are out. Penrose [13], for instance, considers connectivity of random geometric graphs in the unit square. Our results (see Corollary 2) translate into Penrose's setting with essentially no change barring a proper normalization for area. One anticipates, for instance, that more generally the results will carry through to "fat" convex shapes though the question is open.

From hard-sphere communication and sensing models to soft, probabilistic models: The spherical 0–1 communication model in which two nodes can communicate error-free if they lie no further than their common communication radius apart is popular but does not correlate well with real-life instances of wireless networks. In practice the capability of two nodes to communicate depends on a variety of factors such as distance, antenna beam patterns, and the relative positions of the communicating vertices and interferers. In a more realistic model we may replace the hard-sphere model of communication by probabilistic models where the ability of two vertices to communicate with each other is modeled as a probability distribution parametrised by various factors such as antenna orientation, distance, and channel noise. The analysis segues smoothly into such situations though we reserve the details. See Venkatesh [17] for a sketch of these extensions. Similar comments apply to the hard-sphere sensing model.

From independent battery lifetimes with a common parametrised distribution to topology- and protocol-dependent distributions: The assumption that battery lifetime distributions are independent and identically distributed appears to be the most unrealistic. The multihop nature of message transmissions in such settings suggests that battery lifetimes will be correlated. To complicate the picture further, dependencies in battery lifetimes are likely to be significantly impacted both by the network topology and the protocols used. Attempts at relaxing the independent lifetime assumption would be of significant interest though the problem appears to be very hard.

APPENDIX

A. Subdominant Contributions in Single-Vertex Isolation

Assertion 2: The boundary contribution satisfies the asymptotic relation $I_{\text{boundary}} = \mathfrak{o}(n^{-1})$ as $n \to \infty$.

Proof: There are two geometrically distinct regimes in the boundary depending on whether X_i and the origin lie on the same side of the chord joining the intersections of the two circles or whether X_i and the origin are separated by the chord. Two typical situations are illustrated in Fig. 3 where the small circle of radius r has been grossly exaggerated in size to make the details visible. Here X_i is located at point Q.

The contribution of the boundary to the probability integral may hence be further decomposed into $I_{\text{boundary}} = I^{(1)}_{\text{boundary}} + I^{(2)}_{\text{boundary}}$ where

$$I^{(1)}_{\text{boundary}} = \int_{1-r}^{\sqrt{1-r^2}} 2\rho e^{-na_\rho G(t)}\, d\rho$$

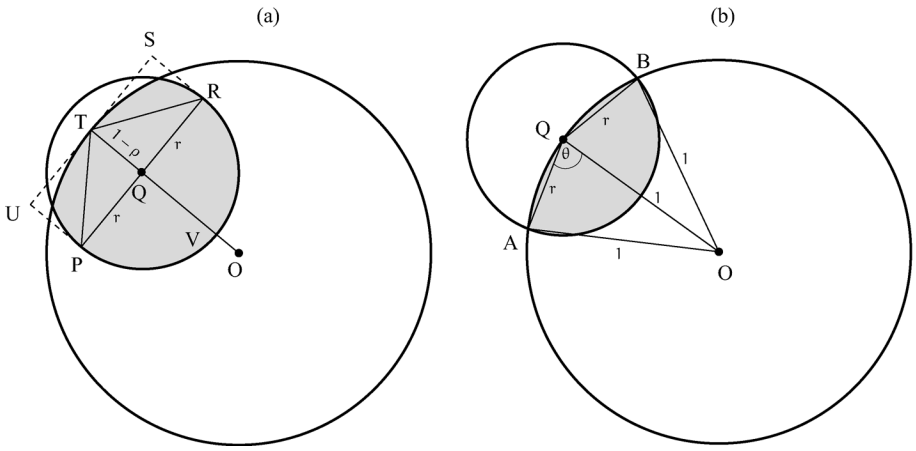

Fig. 3. The boundary regime and the visibility lens (shown shaded) with X_i located at point Q. (a) The vertex is located in the near-boundary $1 - r < \rho \leq \sqrt{1-r^2}$. (b) The vertex is located at the very edge of the far-boundary $\sqrt{1-r^2} < \rho \leq 1$.

and

$$I^{(2)}_{\text{boundary}} = \int_{\sqrt{1-r^2}}^{1} 2\rho e^{-na_\rho G(t)}\, d\rho$$

are the near- and far-boundary contributions, respectively. We consider these in turn.

The near-boundary: $1 - r < \rho \leq \sqrt{1-r^2}$. This is the critical region where the boundary effects are most pronounced. Consider the typical situation illustrated in Fig. 3(a). While the calculation of lens area is now routine, if tedious, we can finesse some of these calculations by bounding the dominant contribution though some care needs to be exercised as the asymptotics are delicate.

On the one hand, the conjoined area encompassed by the semicircle PQRVP and the isosceles triangle PTR is wholly contained within the lens while, on the other, the conjoined area encompassed by the semicircle PQRVP and the rectangle PUSR contains the entire lens. It follows that the area of the lens, A_ρ, is bounded below and above, respectively, by these conjoined areas. An easy calculation now shows that

$$\frac{1}{2}\pi r^2 + r(1-\rho) < A_\rho < \frac{1}{2}\pi r^2 + 2r(1-\rho)$$

and, consequently, the probability $a_\rho = \frac{1}{\pi}A_\rho$ that a randomly placed vertex will land in the lenticular area at the near-boundary is bounded by

$$\frac{1}{2}r^2 + \frac{1}{\pi}r(1-\rho) < a_\rho < \frac{1}{2}r^2 + \frac{2}{\pi}r(1-\rho). \qquad (17)$$

The lower bound for a_ρ may be immediately deployed in bounding the contribution of the near-boundary to the probability integral via

$$\begin{aligned} I^{(1)}_{\text{boundary}} &\overset{\text{(i)}}{\leq} e^{-nr^2G(t)/2} \int_{1-r}^{\sqrt{1-r^2}} 2\rho e^{-nrG(t)(1-\rho)/\pi}\, d\rho \\ &\overset{\text{(ii)}}{\leq} 2e^{-nr^2G(t)/2} \int_{1-r}^{\sqrt{1-r^2}} e^{-nrG(t)(1-\rho)/\pi}\, d\rho \\ &\overset{\text{(iii)}}{=} 2e^{-nr^2G(t)/2} \int_{1-\sqrt{1-r^2}}^{r} e^{-nrG(t)u/\pi}\, du \\ &\leq 2e^{-nr^2G(t)/2} \int_{0}^{\infty} e^{-nrG(t)u/\pi}\, du \\ &= \frac{2\pi e^{-nr^2G(t)/2}}{nrG(t)} \sim \frac{2\pi r\sqrt{\lambda}}{\sqrt{n}\,\log n} \qquad (n \to \infty) \end{aligned}$$

where (i) follows from the lower bound (17) for a_ρ, (ii) holds because ρ is trivially bounded above by $\sqrt{1-r^2} \leq 1$ inside the integral, and (iii) follows from a change of variable of integration from ρ to $u = 1 - \rho$. We hence obtain the asymptotic estimate

$$I^{(1)}_{\text{boundary}} = \mathcal{O}\left(\frac{r}{\sqrt{n}\log n}\right) = \mathfrak{o}\left(\frac{1}{n}\right) \qquad (n \to \infty)$$

by virtue of the growth condition $r = r_n = \mathfrak{o}(\frac{\log n}{\sqrt{n}})$. It follows that the contribution from the near-boundary to the isolation probability is dominated asymptotically by the interior contribution $I_{\text{interior}} \sim \lambda/n$.[5]

The far-boundary: $\sqrt{1-r^2} < \rho \leq 1$. Recall that a_ρ decreases monotonically as ρ increases so that $a_\rho \geq a_1 = \frac{1}{\pi}A_1$ where A_1 is the area of the visibility lens when X_i is situate on the circumference of the unit circle. The situation is illustrated in Fig. 3(b) where the small circle of radius r has again been grossly exaggerated to make visible the geometric detail.

With notation as in Fig. 3(b), $\theta = \angle\text{AQO}$ is the half-angle of the sector enclosed by the chords AQ and BQ and the interior rim of the circle of radius r centered at Q on the circumference of the unit circle. Write A_{sector} for the area of this sector. It follows that $A_{\text{sector}} = \frac{1}{2}(2\theta)r^2 = \theta r^2$. As AOQ is an isosceles triangle with side 1 and base r, we have $\theta = \arccos(\frac{r}{2}) =$

[5]That the rate for r cannot be further increased may be seen from the upper bound for a_ρ in (17). An entirely similar calculation to that above shows indeed that $I^{(1)}_{\text{boundary}} \gtrsim \pi\sqrt{\lambda}/\sqrt{n}\log n$ so that it follows that $I^{(1)}_{\text{boundary}}$ is *exactly* of the asymptotic order of $r/\sqrt{n}\log n$. If $r = r_n$ were to have an asymptotic rate of the order of or higher than $\log n/\sqrt{n}$ then the contribution from the boundary is at least comparable to the interior contribution $I_{\text{interior}} \sim \frac{\lambda}{n}$ and the boundary comes into play.

$\frac{\pi}{2} - \arcsin(\frac{r}{2})$. In consequence of the bound $\arcsin x \le 2x$ for sufficiently small x (Lemma 1(a)), we then obtain

$$\begin{aligned} a_1 &= \frac{1}{\pi}A_1 \ge \frac{1}{\pi}A_{\text{sector}} \\ &= \frac{1}{2}r^2 - \frac{1}{\pi}r^2 \arcsin\left(\frac{r}{2}\right) \ge \frac{1}{2}r^2 - \frac{1}{\pi}r^3 \end{aligned} \tag{18}$$

for all sufficiently large n (recall $r = r_n \to 0$). The far-boundary contribution to the probability integral may hence be bounded by

$$\begin{aligned} I^{(2)}_{\text{boundary}} &= \int_{\sqrt{1-r^2}}^{1} 2\rho e^{-na_\rho G(t)}\, d\rho \\ &\le \int_{\sqrt{1-r^2}}^{1} 2\rho e^{-na_1 G(t)}\, d\rho \\ &= r^2 e^{-na_1 G(t)} \\ &\le r^2 e^{-\frac{1}{2}nr^2 G(t) + \frac{1}{\pi}nr^3 G(t)} \\ &= r^2 e^{-nr^2 G(t)/2}\left[1 + \mathfrak{o}\left(\frac{\log^2 n}{n}\right)\right] \\ &\sim r^2\sqrt{\frac{\lambda}{n}} \qquad (n \to \infty) \end{aligned}$$

leading to the asymptotic estimate

$$I^{(2)}_{\text{boundary}} = \mathcal{O}\left(\frac{r^2}{\sqrt{n}}\right) = \mathfrak{o}\left(\frac{\log^2 n}{n^{3/2}}\right) = \mathfrak{o}\left(\frac{1}{n}\right).$$

From the near- and far-boundary estimates we obtain the entire boundary contribution to the probability integral as $I_{\text{boundary}} = I^{(1)}_{\text{boundary}} + I^{(2)}_{\text{boundary}} = \mathfrak{o}(n^{-1})$.[6] □

B. Subdominant Contributions in Conjunctions of Vertex Isolations

Assertion 4: The asymptotic order relation $J_{k_1,\dots,k_\gamma} = \mathfrak{o}(n^{-k})$ holds for every fixed choice of $k_1, \dots, k_\gamma$ and consequently the contribution from graphs with overlapping regions of visibility satisfies $J_{\text{overlap}} = \mathfrak{o}(n^{-k})$ as $n \to \infty$.

Proof: Begin by considering the cases when the overlap graphs consist of a single component, $\gamma = 1$. Of course, in these cases, the graphs themselves are connected and the single component has size k. As we shall see, this case informs all the others.

Specializing to the case $\gamma = 1$, (12) becomes

$$\begin{aligned} J_k = \sum_{\mathcal{F}_k} \mathbf{E}\big[&1_{\mathbb{C}(\mathcal{F}_k)}(X_1, \dots, X_k) \\ &\times \mathbf{P}\left({}^0L_{1,\dots,k}(t) \mid X_1, \dots, X_k\right)\big] \end{aligned} \tag{19}$$

where $\mathcal{F}_k$ now ranges over all *connected graphs* on k vertices. Consider any connected overlap graph $\mathcal{F}_k$ and the associated equivalence class of k-tuples $\mathbb{C}(\mathcal{F}_k)$. As to any vertex i there is at least one vertex j such that (i,j) is an edge of $\mathcal{F}_k$, it follows that for any k-tuple $(x_1, \dots, x_k) \in \mathbb{C}(\mathcal{F}_k)$, to every point x_i there is at least one other point x_j such that the regions of visibility of x_i and x_j overlap, that is, $|x_i - x_j| \le 2r$. If the proximity of x_i and x_j is such that indeed $|x_i - x_j| \le r$ then vertices X_i and X_j will be adjacent to each other in the original graph $\mathcal{G}_{n,r}$. It follows that, conditioned on $\{X_1 = x_1, \dots, X_k = x_k\}$, the occurrence of the event ${}^0L_{1,\dots,k}(t)$ will require not only that any of the vertices $X_{k+1}, \dots, X_n$ that fall in the conjoined visibility region $\mathbb{V}(x_1) \cup \cdots \cup \mathbb{V}(x_k)$ be extinguished but may also enjoin the extinction of two or more of the vertices X_1 through X_k themselves. But in all cases we may bound

$$\begin{aligned} &\mathbf{P}\left({}^0L_{1,\dots,k}(t) \,|\, X_1 = x_1, \dots, X_k = x_k\right) \\ &\quad \overset{\text{(v)}}{\le} (1 - a_k(x_1, \dots, x_k)G(t))^{n-k} \\ &\quad \overset{\text{(vi)}}{=} \left[1 + \mathcal{O}\left(\frac{\log^2 n}{n}\right)\right] e^{-na_k(x_1,\dots,x_k)G(t)} \end{aligned} \tag{20}$$

where in (v) the inequality takes cognizance of the fact that some of the vertices from X_1 through X_k may be mutually adjacent and (vi) follows from the by-now standard process (5), (6). It follows that

$$\begin{aligned} J_k &\le \left[1 + \mathcal{O}\left(\frac{\log^2 n}{n}\right)\right] \\ &\quad \times \sum_{\mathcal{F}_k} \mathbf{E}\left[1_{\mathbb{C}(\mathcal{F}_k)}(X_1, \dots, X_k) e^{-na_k(X_1,\dots,X_k)G(t)}\right] \\ &= \left[1 + \mathcal{O}\left(\frac{\log^2 n}{n}\right)\right] \\ &\quad \times \mathbf{E}\left[\sum_{\mathcal{F}_k} 1_{\mathbb{C}(\mathcal{F}_k)}(X_1, \dots, X_k) e^{-na_k(X_1,\dots,X_k)G(t)}\right]. \end{aligned}$$

We now begin the process of consolidating all connected overlap graphs under one rubric. Observe that $\sum_{\mathcal{F}_k} 1_{\mathbb{C}(\mathcal{F}_k)}(X_1, \dots, X_k)$ is itself the indicator for all k-tuples $(X_1, \dots, X_k)$ for which the corresponding overlap graph is connected. Accordingly, write $\mathbb{C}_k$ for the subset of k-tuples $(x_1, \dots, x_k)$ in $\mathbb{S}^k$ for which $\mathcal{H}_k(x_1, \dots, x_k)$ is connected. It then follows that $\sum_{\mathcal{F}_k} 1_{\mathbb{C}(\mathcal{F}_k)}(X_1, \dots, X_k) = 1_{\mathbb{C}_k}(X_1, \dots, X_k)$ hence

$$\begin{aligned} J_k \le &\left[1 + \mathcal{O}\left(\frac{\log^2 n}{n}\right)\right] \\ &\times \mathbf{E}\left[1_{\mathbb{C}_k}(X_1, \dots, X_k) e^{-na_k(X_1,\dots,X_k)G(t)}\right]. \end{aligned} \tag{21}$$

We may range over the k-tuples $(x_1, \dots, x_k)$ in $\mathbb{C}_k$ by allowing x_1 to range over the unit disc $\mathbb{S}$ and, for each x_1, allowing the $(k-1)$-tuple $(x_2, \dots, x_k)$ to range over the subset $\mathbb{C}_{k-1}(x_1)$ of $\mathbb{S}^{k-1}$ for which the overlap graph $\mathcal{H}_k(x_1, \dots, x_k)$ remains connected. Now connectivity enjoins that the maximum distance from x_1 to any of the remaining points $x_2, \dots, x_k$ can be no larger than $2(k-1)r$. It follows that $\mathbb{C}_{k-1}(x_1)$ is contained in the set of $(k-1)$-tuples $(x_2, \dots, x_k)$ for which

$$\max_{2 \le i \le k} |x_i - x_1| \le (2k-2)r.$$

These considerations suggest that we introduce a new random variable Z defined by $Z = \max_{2 \le i \le k} |X_i - X_1|$ and representing the *diameter* of the overlap graph as viewed from X_1.

[6] It may be remarked that the analysis for the far-boundary can be applied, essentially without change, to the entire boundary contribution. While the analytical simplification is considerable it is at the cost of the much cruder estimate $r/\sqrt{n}$ for the boundary contribution which will now be small compared to the interior contribution of order $1/n$ only if $r = r_n = \mathfrak{o}(\frac{1}{\sqrt{n}})$. This, alas, is too small a radius of communication to guarantee connectivity and the detailed analysis of the boundary effects appears inescapable.

The game plan is to exploit the fact that large diameter connected graphs have relatively large footprints while small diameter connected graphs are relatively unlikely to occur while retaining bounded footprints. The latter effect is similar in flavor to the balancing act we encountered at the boundary in the analysis for a single vertex. To proceed, we now have

$$\begin{aligned}1_{\mathbb{C}_k}(X_1,\ldots,X_k) &= 1_{\mathbb{S}}(X_1)1_{\mathbb{C}_{k-1}(X_1)}(X_2,\ldots,X_k)\\ &\le 1_{\mathbb{S}}(X_1)1_{[0,(2k-2)r]}(Z)\end{aligned}$$

so that the expectation on the right-hand side of (21) may be bounded by

$$\begin{aligned}&\mathbf{E}\left[1_{\mathbb{C}_k}(X_1,\ldots,X_k)e^{-na_k(X_1,\ldots,X_k)G(t)}\right]\\ &\quad=\mathbf{E}\left[1_{\mathbb{S}}(X_1)\mathbf{E}\left(1_{\mathbb{C}_{k-1}(X_1)}(X_2,\ldots,X_k)\right.\right.\\ &\qquad\left.\left.\times\ e^{-na_k(X_1,\ldots,X_k)G(t)}\,|\,X_1\right)\right]\\ &\quad\le\mathbf{E}\left[1_{\mathbb{S}}(X_1)\mathbf{E}\left(1_{[0,(2k-2)r]}(Z)\right.\right.\\ &\qquad\left.\left.\times e^{-na_k(X_1,\ldots,X_k)G(t)}\,|\,X_1\right)\right].\end{aligned}$$

Now set $j^*=\arg\max_{2\le i\le k}|X_i-X_1|$ and let X_{j^*} be any point at maximal distance Z from X_1. It is clear that the conjoined area of visibility of the points $X_1,\ldots,X_k$ certainly includes the conjoined areas of visibility of the points X_1 and X_{j^*} alone so that $a_k(X_1,\ldots,X_n)\ge a_2(X_1,X_{j^*})$. Substituting on the right-hand side above we may continue to bound the expectation to obtain

$$\begin{aligned}&\mathbf{E}\left[1_{\mathbb{C}_k}(X_1,\ldots,X_k)e^{-na_k(X_1,\ldots,X_k)G(t)}\right]\\ &\quad\le\mathbf{E}\left[1_{\mathbb{S}}(X_1)\mathbf{E}\left(1_{[0,(2k-2)r]}(Z)e^{-na_2(X_1,X_{j^*})G(t)}\,\middle|\,X_1\right)\right]\\ &\quad\triangleq K(n).\end{aligned}\tag{22}$$

The messy problem of estimating $a_k(X_1,\ldots,X_k)$ for a random k-tuple is now reduced to that of estimating $a_2(X_1,X_{j^*})$ for a pair of vertices, albeit with a special statistical structure.

Following the mode of analysis for a single vertex we now partition $\mathbb{S}$ into an interior region $\mathbb{I}=\{x:|x|\le 1-(2k-1)r\}$ and an (expanded) boundary annulus $\mathbb{S}\setminus\mathbb{I}=\{x:1-(2k-1)r<|x|\le 1\}$. Then $1_{\mathbb{S}}(X_1)=1_{\mathbb{I}}(X_1)+1_{\mathbb{S}\setminus\mathbb{I}}(X_1)$ and we may partition the bound $K(n)$ on the right-hand side of (22) further into the sum of the two contributions $K(n)=K_{\text{interior}}+K_{\text{boundary}}$ where

$$\begin{aligned}&K_{\text{interior}}\\ &\quad=\mathbf{E}\left[1_{\mathbb{I}}(X_1)\mathbf{E}\left(1_{[0,(2k-2)r]}(Z)e^{-na_2(X_1,X_{j^*})G(t)}\,\middle|\,X_1\right)\right]\\ &K_{\text{boundary}}\\ &\quad=\mathbf{E}\left[1_{\mathbb{S}\setminus\mathbb{I}}(X_1)\mathbf{E}\right.\\ &\qquad\left.\times\left(1_{[0,(2k-2)r]}(Z)\ e^{-na_2(X_1,X_{j^*})G(t)}\,\middle|\,X_1\right)\right].\end{aligned}\tag{23}$$

We consider these in turn.

The interior overlap contribution: If $X_1\in\mathbb{I}$ then the discs of radius r centered at X_1 and X_{j^*} are both wholly contained within the unit disc. As illustrated in Fig. 4 there are now two possible cases depending on whether the regions of visibility of X_1 and X_{j^*} intersect.

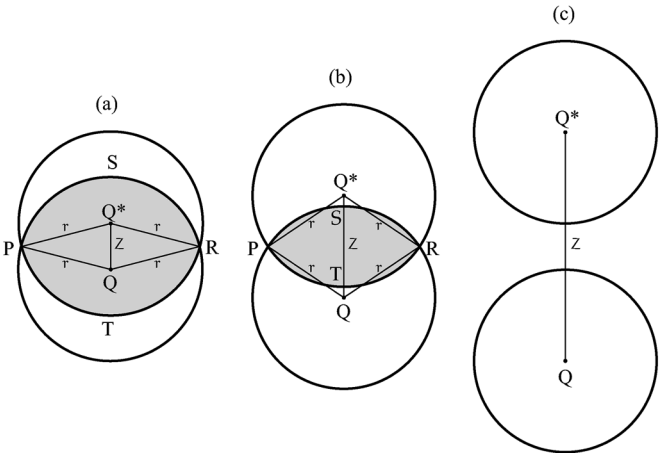

Fig. 4. Point X_1 in the interior $\mathbb{I}$ of the unit circle is located at point Q while point X_{j^*} is located at point Q^*. (a), (b) Two cases where the regions of visibility of X_1 and X_{j^*} overlap. The overlap lens is shown shaded. (c) The regions of visibility of X_1 and X_{j^*} are disjoint.

CASE *1:* When $0\le Z\le 2r$ the regions of visibility of X_1 and X_{j^*} intersect as shown in Figs. 4(a) and (b). Let A_{lens} be the area of the shaded lenticular overlap region shown in the figures. Then $A_2(X_1,X_{j^*})=A_1(X_1)+A_2(X_2)-A_{\text{lens}}=2\pi r^2-A_{\text{lens}}$. Now consider the sector enclosed by the radial lines QP and QR on the one hand and the arc PSR on the other. This sector has half-angle given by $\angle\mathrm{PQQ}^*=\arccos(\frac{Z}{2r})=\frac{\pi}{2}-\arcsin(\frac{Z}{2r})$. It follows that the sector has area $A_{\text{sector}}=r^2\angle\mathrm{PQQ}^*=\frac{\pi}{2}r^2-r^2\arcsin(\frac{Z}{2r})$. By symmetry, the sector enclosed by the radial lines Q^*P and Q^*R and the arc PTR also has area A_{sector}. The sum of the areas of these two sectors exceeds the area of the overlap lens exactly by the area of the rhombus PQRQ^*. While an exact calculation is not difficult we can afford to be a little cavalier here with the bound $A_{\text{lens}}\le 2A_{\text{sector}}=\pi r^2-2r^2\arcsin(\frac{Z}{2r})$. We hence obtain

$$A_2(X_1,X_{j^*})\ge\pi r^2+2r^2\arcsin\left(\frac{Z}{2r}\right)\ge\pi r^2+rZ$$

by virtue of the bound $\arcsin x\ge x$ (Lemma 1). In consequence

$$a_2(X_1,X_{j^*})=\frac{1}{\pi}A_2(X_1,X_{j^*})\ge r^2+\frac{1}{\pi}rZ.$$

CASE 2: When $2r<Z\le(2k-2)r$ the regions of visibility of X_1 and X_{j^*} are disjoint (Fig. 4(c)) and $A_2(X_1,X_{j^*})=A_1(X_1)+A_1(X_{j^*})=2\pi r^2$ whence $a_2(X_1,X_{j^*})=2r^2$.

Write $F(z\,|\,X_1)$ and $f(z\,|\,X_1)$ for the conditional distribution function and density, respectively, of Z given X_1. Then for all $0\le z\le 1-|X_1|$, the circle of radius z centered at X_1 is wholly contained within the unit circle so that the conditional distribution satisfies $F(z\,|\,X_1)=\mathbf{P}\{Z\le z\,|\,X_1\}=\mathbf{P}\{|X_2-X_1|\le z,\ldots,|X_k-X_1|\le z\,|\,X_1\}=(z^2)^{k-1}$ as the distances $|X_i-X_1|$ $(2\le i\le k)$ are conditionally independent given X_1; the corresponding conditional density is $f(z\,|\,X_1)=(2k-2)z^{2k-3}$. In particular, for all $X_1\in\mathbb{I}$, the conditional distribution and density of Z satisfy $F(z\,|\,X_1)=z^{2k-2}$

and $f(z\,|\,X_1) = (2k-2)z^{2k-3}$ for $0 \le z \le (2k-2)r$. Putting the pieces together, for $X_1 \in \mathbb{I}$,

$$\begin{aligned}
&\mathbf{E}\left(1_{[0,(2k-2)r]}(Z)e^{-na_2(X_1,X_{J^*})G(t)}\,|\,X_1\right)\\
&\quad=\mathbf{E}\left(1_{[0,2r]}(Z)e^{-na_2(X_1,X_{J^*})G(t)}\,|\,X_1\right)\\
&\qquad+\mathbf{E}\left(1_{(2r,(2k-2)r]}(Z)e^{-na_2(X_1,X_{J^*})G(t)}\,|\,X_1\right)\\
&\quad\le e^{-nr^2G(t)}\int_0^{2r}(2k-2)z^{2k-3}e^{-nrzG(t)/\pi}\,dz\\
&\qquad+e^{-2nr^2G(t)}\mathbf{P}\{2r<Z\le(2k-2)r\,|\,X_1\}\\
&\quad\le(2k-2)e^{-nr^2G(t)}\int_0^{\infty}z^{2k-3}e^{-nrzG(t)/\pi}\,dz\\
&\qquad+e^{-2nr^2G(t)}\mathbf{P}\{Z\le(2k-2)r\,|\,X_1\}\\
&\quad=\pi^{2k-2}(2k-2)!\frac{r^{2k-2}e^{-nr^2G(t)}}{(nr^2G(t))^{2k-2}}\\
&\qquad+(2k-2)^{2k-2}r^{2k-2}e^{-2nr^2G(t)}\\
&\quad=\mathcal{O}\left(\frac{r^{2k-2}}{n\log^{2k-2}n}+\frac{r^{2k-2}}{n^2}\right)\\
&\quad=\mathcal{O}\left(\frac{r^{2k-2}}{n\log^{2k-2}n}\right)
\end{aligned}$$

where the order bounds are again uniform in X_1. As $\mathbf{E}(1_{\mathbb{I}}(X_1)) = \mathbf{P}\{|X_1| \le 1-(2k-1)r\} = [1-(2k-1)r]^2 = 1+\mathcal{O}(r)$, substitution in (23) yields

$$K_{\text{interior}} = \mathcal{O}\left(\frac{r^{2k-2}}{n\log^{2k-2}n}\right) = \mathfrak{o}\left(\frac{1}{n^k}\right) \tag{24}$$

which is sub-dominant, if barely, compared to the nonoverlap contribution $J_{\text{nonoverlap}} \sim \lambda^k/n^k$ asymptotically as $n\to\infty$.

The boundary overlap contribution: As was the case for a single vertex, the calculations in the near-boundary are delicate and a careful case-by-case analysis is unavoidable. Write $1_{[0,(2k-2)r]}(Z) = 1_{[0,2r]}(Z) + 1_{(2r,(2k-2)r]}(Z)$ so that the expression for K_{boundary} in (23) can be written as the sum of two terms, one for *proximate* $Z \le 2r$ when the visibility region of X_1 overlaps with that of each of X_2 through X_k and the other for *well-separated* $Z > 2r$ when the two points X_1 and X_{J^*} are not adjacent in the overlap graph. We begin by disposing of the latter case first.

Well-separated Z: If $Z > 2r$ then $a_2(X_1, X_{J^*}) = a_1(X_1) + a_1(X_{J^*})$ as the visibility regions of X_1 and X_{J^*} do not overlap (even though there is a chain of overlaps connecting them in the overlap graph). The lower bound for a_1 in (18) shows then that $a_2(X_1, X_{J^*}) \ge r^2 - \frac{2}{\pi}r^3$ for all sufficiently large n while, as seen above, $\mathbf{P}\{2r < Z \le (2k-2)r\,|\,X_1\} \le [(2k-2)r]^{2(k-1)}$ and $\mathbf{E}(1_{\mathbb{S}\setminus\mathbb{I}}(X_1)) = 1-\mathbf{P}\{|X_1| \le 1-(2k-1)r\} \le (4k-2)r$. Hence, we obtain the asymptotic estimate

$$\begin{aligned}
&\mathbf{E}\left[1_{\mathbb{S}\setminus\mathbb{I}}(X_1)\mathbf{E}\left(1_{(2r,(2k-2)r]}(Z)e^{-na_2(X_1,X_{J^*})G(t)}\,|\,X_1\right)\right]\\
&\quad\le(4k-2)(2k-2)^{2k-2}r^{2k-1}e^{-nr^2G(t)+2nr^3G(t)/\pi}\\
&\quad=\mathcal{O}\left(\frac{r^{2k-1}}{n}\right)=\mathfrak{o}\left(\frac{\log^{2k-1}n}{n^{k+1/2}}\right)=\mathfrak{o}\left(\frac{1}{n^k}\right)
\end{aligned} \tag{25}$$

which, like the interior overlap contribution, is subdominant.

Proximate Z: We are left with the principal boundary overlap contributions arising from the regime $X_i \in \mathbb{S}\setminus\mathbb{I}$ and $Z \le 2r$. As X_1 varies over the boundary $\mathbb{S}\setminus\mathbb{I}$, three regions may be identified: 1) the *very-near-boundary*, $1-(2k-1)r < |X_1| \le 1-r$, when the disc of radius r centered at X_1 is completely contained within the unit disc; 2) the *near-boundary*, $1-r < |X_1| \le \sqrt{1-r^2}$, as seen for a single vertex when part of the disc $\mathbb{D}(r;X_1)$ is lost to the visibility region due to intersection with the boundary; and 3) the *far-boundary*, $\sqrt{1-r^2} < |X_1| \le 1$, also as seen in the analysis for a single vertex when the area of the visibility region of X_1 is approximately $\frac{1}{2}\pi r^2$. Accordingly, write

$$\begin{aligned}
1_{\mathbb{S}\setminus\mathbb{I}}(X_1) = {}& 1_{(1-(2k-1)r,1-r]}(|X_1|)\\
&+1_{(1-r,\sqrt{1-r^2}]}(|X_1|)+1_{(\sqrt{1-r^2},1]}(|X_1|)
\end{aligned}$$

and partition the range of X_1 to obtain

$$\begin{aligned}
&\mathbf{E}\left[1_{\mathbb{S}\setminus\mathbb{I}}(X_1)\mathbf{E}\left(1_{[0,2r]}(Z)e^{-na_2(X_1,X_{J^*})G(t)}\,|\,X_1\right)\right]\\
&\qquad=B^{(\text{i})}_{\text{boundary}}+B^{(\text{ii})}_{\text{boundary}}+B^{(\text{iii})}_{\text{boundary}}
\end{aligned} \tag{26}$$

where $B^{(\text{i})}_{\text{boundary}}$ is the contribution from the very-near-boundary, $B^{(\text{ii})}_{\text{boundary}}$ is the contribution from the near-boundary, and $B^{(\text{iii})}_{\text{boundary}}$ is the contribution from the far-boundary.

Before proceeding further it will be useful to make two key observations at this point that will help to substantially simplify the calculations.

KEY OBSERVATION 1: *The conditional density* of Z *given* X_1 *has the uniform envelope* $f(z\,|\,X_1) \le (2k-2)z^{2k-3}$ *for all* $z \ge 0$. Indeed, for any $i \ne 1$, the conditional distribution of $|X_i - X_1|$ given X_1 is bounded by

$$\begin{aligned}
&\mathbf{P}\{|X_i-X_1|\le z\,|\,X_1\}\\
&\qquad=\frac{1}{\pi}\int_{\mathbb{D}(z;X_1)\cap\mathbb{S}}dx\le\frac{1}{\pi}\int_{\mathbb{D}(z;X_1)}dx=z^2
\end{aligned}$$

for all $z \ge 0$ and it follows similarly that, for any $\epsilon > 0$

$$\begin{aligned}
&\mathbf{P}\{z<|X_i-X_1|\le z+\epsilon\,|\,X_1\}\\
&\quad=\frac{1}{\pi}\int_{\mathbb{D}(z+\epsilon;X_1)\setminus\mathbb{D}(z;X_1)\cap\mathbb{S}}dx\\
&\quad\le\frac{1}{\pi}\int_{\mathbb{D}(z+\epsilon;X_1)\setminus\mathbb{D}(z;X_1)}dx\\
&\quad=(z+\epsilon)^2-z^2=2z\epsilon+\epsilon^2
\end{aligned}$$

as the intersection with the unit circle of the annulus of width ϵ at the boundary of the circle of radius z centered at X_1 has area certainly no larger than that of the annulus itself. For convenience, introduce the notational shorthand $F_2 = \mathbf{P}\{|X_i - X_1| \le z\}$ and $\Delta F_2 = \mathbf{P}\{z < |X_i - X_1| \le z+\epsilon\,|\,X_1\}$. As the event $\{z < Z \le z+\epsilon\}$ occurs if, and only if, for some $j \ge 1$, exactly j of the X_i $(2 \le i \le k)$ satisfy $z < |X_i - X_1| \le z+\epsilon$ with the remaining $k-1-j$ of the X_i satisfying $|X_i - X_j| \le z$ it follows that

$$\begin{aligned}
&\frac{1}{\epsilon}[F(z+\epsilon\,|\,X_1)-F(z\,|\,X_1)]\\
&\quad=\frac{1}{\epsilon}\mathbf{P}\{z<Z\le z+\epsilon\,|\,X_1\}
\end{aligned}$$

$$= \frac{1}{\epsilon}\sum_{j=1}^{k-1}\binom{k-1}{j} F_2^{k-1-j}[\Delta F_2]^j$$
$$\leq \frac{1}{\epsilon}\sum_{j=1}^{k-1}\binom{k-1}{j} z^{2k-2-2j}(2z\epsilon+\epsilon^2)^j$$
$$= \sum_{j=1}^{k-1}\binom{k-1}{j} z^{2k-2-2j}\epsilon^{j-1}(2z+\epsilon)^j.$$

Allowing ϵ to tend to zero on both sides of the bound we obtain $f(z\,|\,X_1) \leq (2k-2)z^{2k-3}$ as claimed.

KEY OBSERVATION 2: *For given X_1 and Z, $a_2(X_1, X_{J^*})$ attains its minimum value when X_{J^*} is situated as closely as possible to the periphery of the unit disc*. In particular, if $Z \leq 1 - |X_1|$ this is occasioned when X_{J^*} lies on the ray from the origin through the point X_1 and athwart X_1 and the circumference of the unit circle. And if $Z > 1 - |X_1|$ this is occasioned when X_{J^*} is one of the two points on the circumference of the unit circle at distance Z from X_1. The validity of the observation may be seen as a consequence of the convexity of the circle whence $\mathbb{D}(r; X_{J^*}) \setminus \mathbb{D}(r; X_1)$ has its minimum area of overlap with the unit disc when X_{J^*} is situate on the point(s) on the circumference of the circle of radius Z centered at X_1 which is closest to the periphery of the unit disc. This observation is key as it allows us to repeatedly leverage our analysis for a single vertex.

The very-near-boundary: $1-(2k-1)r < |X_1| \leq 1-r$. The simplest bounds suffice here. It is trivial that $A_2(X_1, X_{J^*}) \geq A_1(X_1) = \pi r^2$ so that $a_2(X_1, X_{J^*}) \geq r^2$. We hence obtain

$$\begin{aligned}
&B^{(\mathrm{i})}_{\mathrm{boundary}}\\
&\leq e^{-nr^2G(t)}\mathbf{E}\left[1_{(1-(2k-1)r,1-r]}(|X_1|)\mathbf{P}\{Z \leq 2r\,|\,X_1\}\right]\\
&\leq e^{-nr^2G(t)}(4r^2)^{k-1}\mathbf{P}\{1-(2k-1)r < |X_1| \leq 1-r\}\\
&= e^{-nr^2G(t)}4^{k-1}r^{2k-2}[(1-r)^2-(1-(2k-1)r)^2]\\
&\leq 4^k(k-1)r^{2k-1}e^{-nr^2G(t)}\\
&= \mathcal{O}\left(\frac{r^{2k-1}}{n}\right) = \mathfrak{o}\left(\frac{\log^{2k-1}n}{n^{k+1/2}}\right) = \mathfrak{o}\left(\frac{1}{n^k}\right) \qquad (27)
\end{aligned}$$

which is easily subdominant with respect to the main contribution from the interior.

The near-boundary: $1-r < |X_1| \leq \sqrt{1-r^2}$. As in the case of a single vertex, the situation is most delicate here and requires careful estimates. As Z varies from 0 to $2r$ two regions may be identified: 1) $0 \leq Z \leq 1-|X_1|$ where the smallest value of $a_2(X_1, X_{J^*})$ occurs when X_{J^*} lies on the ray outward from the origin through the point X_1, and 2) $1-|X_1| < Z \leq 2r$ when the smallest value of $a_2(X_1, X_{J^*})$ occurs when X_{J^*} is on the circumference of the unit circle at a distance Z from X_1. The key to the analysis of both cases is identifying suitable bounds for $a_2(X_1, X_{J^*})$ *explicitly as functions of* $1-|X_1|$ *and* Z.

i) X_{J^*} is colinear with X_1 and the origin. In the worst case, X_{J^*} is pinched into the narrow region between X_1 and the circumference of the unit disc and the worst-case area of the conjoined visibility region of X_1 and X_{J^*} will in consequence not be much larger than that of X_1 alone. But this is sufficient as we see next.

Leveraging our results for a single vertex we obtain

$$a_2(X_1, X_{J^*}) \geq a_1(X_1) \geq \frac{1}{2}r^2 + \frac{1}{\pi}r(1-|X_1|)$$

by an appeal to (17). Consequently

$$\begin{aligned}
&\mathbf{E}\left[1_{(1-r,\sqrt{1-r^2}]}(|X_1|)\right.\\
&\quad\left.\times\,\mathbf{E}\left(1_{[0,1-|X_1|]}(Z)e^{-na_2(X_1,X_{J^*})G(t)}\,|\,X_1\right)\right]\\
&\overset{\text{(vii)}}{\leq} 2(2k-2)e^{-nr^2G(t)/2}\int_{1-r}^{\sqrt{1-r^2}}\mathrm{d}\rho\,\rho e^{-nr(1-\rho)G(t)/\pi}\\
&\quad\times\int_0^{1-\rho}dz\,z^{2k-3}\\
&\overset{\text{(viii)}}{\leq} 2e^{-nr^2G(t)/2}\int_{1-r}^{\sqrt{1-r^2}}(1-\rho)^{2k-2}\\
&\quad\times e^{-nr(1-\rho)G(t)/\pi}\,d\rho\\
&\overset{\text{(ix)}}{=} \frac{2\pi^{2k-1}e^{-nr^2G(t)/2}}{(nrG(t))^{2k-1}}\int_{nrG(t)(1-\sqrt{1-r^2})/\pi}^{nr^2G(t)/\pi}u^{2k-2}e^{-u}\,du\\
&\leq \frac{2\pi^{2k-1}e^{-nr^2G(t)/2}}{(nrG(t))^{2k-1}}\int_0^{\infty}u^{2k-2}e^{-u}\,du\\
&= 2\pi^{2k-1}\frac{2k-2)!r^{2k-1}e^{-nr^2G(t)/2}}{(nr^2G(t))^{2k-1}}\\
&= \mathcal{O}\left(\frac{r^{2k-1}}{\sqrt{n}\log^{2k-1}n}\right) = \mathfrak{o}\left(\frac{1}{n^k}\right) \qquad (28)
\end{aligned}$$

where (vii) follows from the key observation that the conditional density of Z has an envelope, in (viii) we use the fact that $\rho \leq \sqrt{1-r^2} < 1$ inside the integral, and (ix) follows from the change of variable of integration to $u = nr(1-\rho)G(t)/\pi$.

(ii) X_{J^*} is on the periphery. The situation is somewhat more complex here as, even in the worst-case, X_{J^*} situated on the circumference of the unit disc starts contributing more significantly to the conjoined region of visibility. Two cartoon figures illustrating this situation are shown in Fig. 5. An arc of the circumference of the unit disc is shown passing through X_{J^*} situated at the point Q* in Fig. 5(a). On the scale of the radius r of the region of visibility, the intersection of the circumference of the unit disc with the circles of radius r at Q and Q* is almost a straight line as shown in (a). In order to make the critical region more visible the curvature of the sensor field vis à vis the regions of visibility has been much exaggerated in Fig. 5(b) where X_1 is situated at point Q and X_{J^*} at a distance $Z > 1-|X_1|$ from X_1 is located on the circumference of the sensor field at point Q*. We take our notation from this figure.

The right-angle triangle PQU whose base PQ has length r and height QU has length $1-|X_1|$, the sector PQR of angle $\pi/2+\theta$ of the circle of radius r at Q, and the sector RQ^*S of angle ϕ of the circle of radius r at Q* are nonoverlapping and contained wholly within the conjoined visibility region $\mathbb{V}(X_1) \cup \mathbb{V}(X_{J^*})$. It follows that

$$A_2(X_1, X_{J^*}) \geq \frac{1}{2}r(1-|X_1|) + \frac{1}{2}r^2\left(\frac{\pi}{2}+\theta\right) + \frac{1}{2}r^2\phi.$$

Elementary calculations now serve to determine the various angles of interest.

1) Let Z' denotes the length of the line segment UQ^*. As two sides of a triangle are larger than the third, a consideration

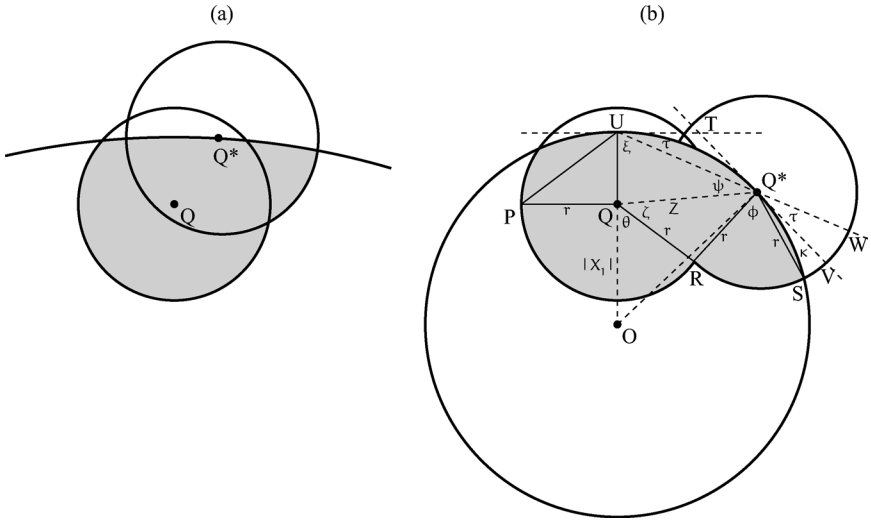

Fig. 5. The near-boundary regime $1-r<|X_1|\le\sqrt{1-r^2}$ for proximate Z satisfying $1-|X_1|<Z\le 2r$. The point X_1 is situate at Q with X_{j^*} at Q* on the periphery of the sensor field. The conjoined region of visibility is shown shaded.

of triangle QUQ* shows that $Z'\le Z+(1-|X_1|)\le 3r$ as $Z\le 2r$ and $1-|X_1|<r$.

2) As UOQ* is an isosceles triangle with sides of length 1 and base of length Z', we have $\xi=\angle\mathrm{OUQ}^*=\arccos(\frac{Z'}{2})=\frac{\pi}{2}-\arcsin(\frac{Z'}{2})$.
3) As UT is the tangent line at $U,\tau=\angle\mathrm{TUQ}^*=\frac{\pi}{2}-\xi=\arcsin(\frac{Z'}{2})\le Z'\le 3r$ for large enough n by virtue of the upper bound for the arcsine function from Lemma 1. With TQ*V the tangent line at Q*, note that τ may also be identified with $\angle\mathrm{VQ}^*\mathrm{W}$.
4) As QRQ* is an isosceles triangle with sides r and base Z, we have $\zeta=\angle\mathrm{RQQ}^*=\angle\mathrm{RQ}^*\mathrm{Q}=\frac{\pi}{2}-\arcsin(\frac{Z}{2r})\le\frac{\pi}{2}-\frac{Z}{2r}$, by virtue of the lower bound for the arcsine function this time, again from Lemma 1.
5) With $\kappa=\angle\mathrm{SQ}^*\mathrm{V}$, the development leading up to (18) in the analysis of the far-boundary for a single vertex shows that $r^2(\frac{\pi}{2}-\kappa)\ge\frac{\pi}{2}r^2-r^3$ so that $\kappa\le r$.
6) With $\psi=\angle\mathrm{QQ}^*U$, it follows that $\phi=\pi-\psi-\zeta-\kappa-\tau\ge\frac{\pi}{2}-\psi+\frac{Z}{2r}-4r$.
7) And finally, an examination of the exterior angle of the triangle UQQ* shows that $\theta+\zeta=\xi+\psi$ so that $\theta=\frac{\pi}{2}-\tau+\psi-\zeta\ge\psi+\frac{Z}{2r}-3r$.

Proceeding with bounding the area of the conjoined region of visibility, we have

$$\begin{aligned}A_2(X_1,X_{j^*})&\ge\frac{1}{2}r(1-|X_1|)+\frac{1}{2}r^2\left(\frac{\pi}{2}+\theta+\phi\right)\\&\ge\frac{1}{2}\pi r^2+\frac{1}{2}r(1-|X_1|)+\frac{1}{2}rZ-\frac{7}{2}r^3\end{aligned}$$

and, in consequence

$$a_2(X_1,X_{j^*})\ge\frac{1}{2}r^2+\frac{1}{2\pi}r(1-|X_1|)+\frac{1}{2\pi}rZ-\frac{7}{2\pi}r^3.$$

Again exploiting the fact that the conditional density of Z has a uniform envelope, we obtain

$$\begin{aligned}&\mathbf{E}\left[1_{(1-r,\sqrt{1-r^2}]}(|X_1|)\right.\\&\quad\left.\times\mathbf{E}\left(1_{(1-|X_1|,2r]}(Z)e^{-na_2(X_1,X_{j^*})G(t)}\,|\,X_1\right)\right]\\&\le 2(2k-2)e^{-\frac{1}{2}nr^2G(t)+\frac{7}{2\pi}nr^3G(t)}\\&\quad\times\int_{1-r}^{\sqrt{1-r^2}}d\rho\,\rho e^{-nr(1-\rho)G(t)/2\pi}\\&\quad\times\int_{1-\rho}^{2r}dz\,z^{2k-3}e^{-nrzG(t)/2\pi}.\end{aligned}$$

Finish off by bounding the inner integral first

$$\begin{aligned}\int_{1-\rho}^{2r}z^{2k-3}e^{-nrzG(t)/2\pi}\,dz&\le\int_0^{\infty}z^{2k-3}e^{-nrzG(t)/2\pi}\,dz\\&=\frac{(2k-3)!(2\pi)^{2k-2}}{(nrG(t))^{2k-2}}\end{aligned}$$

then the outer integral,

$$\begin{aligned}&\int_{1-r}^{\sqrt{1-r^2}}2\rho e^{-nr(1-\rho)G(t)/2\pi}\,d\rho\\&\quad\le 2\int_{1-\sqrt{1-r^2}}^{r}e^{-nruG(t)/2\pi}\,du\\&\quad\le 2\int_0^{\infty}e^{-nruG(t)/2\pi}\,du=\frac{4\pi}{nrG(t)}\end{aligned}$$

via the change of variable of integration $u\leftarrow 1-\rho$, to finally obtain the bound

$$\begin{aligned}&\mathbf{E}\left[1_{(1-r,\sqrt{1-r^2}]}(|X_1|)\right.\\&\quad\left.\times\,\mathbf{E}\left(1_{(1-|X_1|,2r]}(Z)e^{-na_2(X_1,X_{j^*})G(t)}\,|\,X_1\right)\right]\\&\le 2^{2k}\pi^{2k-1}(2k-2)!\frac{r^{2k-1}e^{-\frac{1}{2}nr^2G(t)+\frac{7}{2\pi}nr^3G(t)}}{(nr^2G(t))^{2k-1}}\\&=\mathcal{O}\left(\frac{r^{2k-1}}{\sqrt{n}\,\log^{2k-1}n}\right)=\mathfrak{o}\left(\frac{1}{n^k}\right).\end{aligned}\tag{29}$$

Mop up by putting (28) and (29) together to get

$$\begin{aligned}&B^{(\mathrm{ii})}_{\mathrm{boundary}}\\&\quad=\mathbf{E}\left[1_{(1-r,\sqrt{1-r^2}]}(|X_1|)\right.\\&\qquad\left.\times\,\mathbf{E}\left(1_{[0,2r]}(Z)e^{-na_2(X_1,X_{j^*})G(t)}\,|\,X_1\right)\right]\\&\quad=\mathcal{O}\left(\frac{r^{2k-1}}{\sqrt{n}\,\log^{2k-1}n}\right)=\mathfrak{o}\left(\frac{1}{n^k}\right)\end{aligned}\tag{30}$$

which is again of the requisite asymptotic order, though barely so for the given rate of $r = r_n$.

The far-boundary: $\sqrt{1-r^2} < |X_1| \leq 1$. Borrowing again from the analysis for a single vertex, we have from (18) that $a_2(X_1, X_{j^*}) \geq a_1(X_1) \geq \frac{1}{2}r^2 - \frac{1}{\pi}r^3$ for sufficiently large n. It follows that

$$\begin{aligned}
&\mathrm{B}^{(\mathrm{iii})}_{\mathrm{boundary}} \\
&\quad = \mathbf{E}\left[1_{(\sqrt{1-r^2},1]}(|X_1|)\right. \\
&\qquad \left.\times \mathbf{E}\left(1_{[0,2r]}(Z)e^{-na_2(X_1,X_{j^*})G(t)} \,|\, \mathrm{X}_1\right)\right] \\
&\quad \leq e^{-\frac{1}{2}nr^2G(t)+\frac{1}{\pi}nr^3G(t)} \\
&\qquad \times \mathbf{E}\left[1_{(\sqrt{1-r^2},1]}(|X_1|)\mathbf{P}\{Z \leq 2r \,|\, X_1\}\right] \\
&\quad \leq e^{-\frac{1}{2}nr^2G(t)+\frac{1}{\pi}nr^3G(t)}(4r^2)^{k-1}\mathbf{P}\{\sqrt{1-r^2} < |X_1| \leq 1\} \\
&\quad \leq e^{-\frac{1}{2}nr^2G(t)+\frac{1}{\pi}nr^3G(t)}(4r^2)^{k-1}\left[1-(1-r^2)\right] \\
&\quad = \mathcal{O}\left(\frac{r^{2k}}{\sqrt{n}}\right) = \mathfrak{o}\left(\frac{\log^{2k} n}{n^{k+1/2}}\right) = \mathfrak{o}\left(\frac{1}{n^k}\right) \qquad (31)
\end{aligned}$$

which is also asymptotically subdominant.

Finale. We can now trace our way back to the starting point. Stitching the boundary contributions for proximate Z together in (26) we have from (27), (30), and (31) that

$$\begin{aligned}
\mathbf{E}\left[1_{\mathbb{S}\setminus B^{(\mathrm{i})}_{\mathrm{boundary}}}(X_1)\mathbf{E}\left(1_{[0,2r]}(Z)e^{-na_2(X_1,X_{j^*})G(t)} \,|\, X_1\right)\right] \\
= \mathfrak{o}\left(n^{-k}\right)
\end{aligned}$$

which together with the estimate (25) when Z is well-separated implies that $K_{\mathrm{boundary}} = \mathfrak{o}(n^{-k})$ in (23), which, in turn, in conjunction with the corresponding estimate (24) for K_{interior} yields $K(n) = K_{\mathrm{interior}} + K_{\mathrm{boundary}} = \mathfrak{o}(n^{-k})$, which then implies in (22) that

$$\mathbf{E}\left[1_{\mathbb{C}_k}(X_1, \ldots, X_k)e^{-na_k(X_1,\ldots,X_k)G(t)}\right] = \mathfrak{o}(n^{-k}). \quad (32)$$

At long last the weariest river winds its way safely to sea. The last estimate returns us finally to (21) and (19) from which we conclude that $J_k = \mathfrak{o}(n^{-k})$ and the contribution due to connected overlap graphs is asymptotically subdominant.

Overlapping regions of visibility, conclusion. Return to the system of (12), (12′) reproduced here for convenience. The contribution from all overlap graphs $\mathcal{F} \neq \mathcal{F}_*$ to the probability of the event that vertices X_1 through X_k are all isolated by time t is

$$J_{\mathrm{overlap}} = \sum_{\gamma=1}^{k-1} \sum_{\substack{k_1 \geq \cdots \geq k_\gamma \geq 1 \\ k_1+\cdots+k_\gamma = k}} J_{k_1,\ldots,k_\gamma}$$

where $J_{k_1,\ldots,k_\gamma}$ is the total contribution from all overlap graphs $\mathcal{F}_{k_1,\ldots,k_\gamma}$ with exactly γ components of sizes $k_1, \ldots, k_\gamma$ and is given by

$$\begin{aligned}
J_{k_1,\ldots,k_\gamma} = \sum_{\mathcal{F}_{k_1,\ldots,k_\gamma}} \mathbf{E}\Big[1_{\mathbb{C}(\mathcal{F}_{k_1,\ldots,k_\gamma})}(X_1, \ldots, X_k) \\
\times \mathbf{P}\left({}^0L_{1,\ldots,k}(t) \,|\, X_1, \ldots, X_k\right)\Big].
\end{aligned}$$

Some algebraic simplification in the expression for $J_{k_1,\ldots,k_\gamma}$ can be achieved by observing that as the points $X_1, \ldots, X_n$ are generated by independent sampling from the uniform distribution on the unit disc, it follows by symmetry that any two overlap graphs $\mathcal{F}_{k_1,\ldots,k_\gamma}$ and $\mathcal{F}'_{k_1,\ldots,k_\gamma}$ that differ only in a permutation of the vertices will contribute exactly the same amount to the sum for $J_{k_1,\ldots,k_\gamma}$. As there are exactly $k!/(k_1!\ldots k_\gamma!)$ allocations of the vertices from X_1 to X_k into γ cells with respective occupancies $k_1, \ldots, k_\gamma$, it follows that

$$\begin{aligned}
J_{k_1,\ldots,k_\gamma} \\
= \frac{k!}{k_1!\ldots k_\gamma!} \sum_{\mathcal{F}_{k_1,\ldots,k_\gamma}}{}' \mathbf{E}\Big[1_{\mathbb{C}(\mathcal{F}_{k_1,\ldots,k_\gamma})}(X_1, \ldots, X_k) \\
\times \mathbf{P}\left({}^0L_{1,\ldots,k}(t) \,|\, X_1, \ldots, X_k\right)\Big]
\end{aligned}$$

where the sum $\sum'$ is now restricted to overlap graphs $\mathcal{F}_{k_1,\ldots,k_\gamma}$ for which the first component consists of the first k_1 vertices $\{X_1, \ldots, X_{k_1}\}$, the second component consists of the next k_2 vertices $\{X_{k_1+1}, \ldots, X_{k_1+k_2}\}$, and so on, with the γth component consisting of the final k_γ vertices $\{X_{k-k_\gamma+1}, \ldots, X_k\}$. As in the case of the connected overlap graphs we now proceed to further consolidate these graphs.

Write $\mathbb{C}_{k_1,\ldots,k_\gamma}$ for the subset of k-tuples $(X_1, \ldots, X_k)$ for which the corresponding overlap graph is divided into γ components with the first component comprised of the vertices $\{X_1, \ldots, X_{k_1}\}$, the second component of the vertices $\{X_{k_1+1}, \ldots, X_{k_1+k_2}\}$, and so on, with the γth component consisting of the vertices $\{X_{k-k_\gamma+1}, \ldots, X_k\}$. It is then clear that the sum $\sum'_{\mathcal{F}_{k_1,\ldots,k_\gamma}} 1_{\mathbb{C}(\mathcal{F}_{k_1,\ldots,k_\gamma})}(X_1, \ldots, X_k)$ is itself the indicator for the set $\mathbb{C}_{k_1,\ldots,k_\gamma}$ and consequently

$$\begin{aligned}
J_{k_1,\ldots,k_\gamma} = \frac{k!}{k_1!\ldots k_\gamma!}\mathbf{E}\Big[1_{\mathbb{C}_{k_1,\ldots,k_\gamma}}(X_1, \ldots, X_k) \\
\times \mathbf{P}\left({}^0L_{1,\ldots,k}(t) \,|\, X_1, \ldots, X_k\right)\Big].
\end{aligned}$$

One final piece of notation to help compact expressions: for $j = 1, \ldots, \gamma$, introduce the nonce notation $x^{(j)} = (x_{k_1+\cdots+k_{j-1}+1}, \ldots, x_{k_1+\cdots+k_j})$ to indicate the jth subsequence of length k_j and, mirroring the notation introduced for connected overlap graphs, let $\mathbb{C}_{k_j}$ denote the set of k_j-tuples $x^{(j)}$ in $\mathbb{S}^{k_j}$ for which the overlap graph $\mathcal{H}_{k_j}(x^{(j)})$ is connected. We may now range through the k-tuples $(x_1, \ldots, x_k)$ comprising the set $\mathbb{C}_{k_1,\ldots,k_\gamma}$ recursively as follows:

BASE: The k_1-tuple $x^{(1)}$ is allowed to range over the subset $\mathbb{C}^{(1)}_{k_1} = \mathbb{C}_{k_1}$ of $\mathbb{S}^{k_1}$ for which the overlap graph $\mathcal{H}_{k_1}(x^{(1)})$ is connected.

RECURRENCE: As j ranges from 2 to γ, for every selection of $x_1, \ldots, x_{k_1+\cdots+k_{j-1}}$, the k_j-tuple $x^{(j)}$ is allowed to range over the subset $\mathbb{C}^{(j)}_{k_j} = \mathbb{C}_{k_j} \setminus (\bigcup_{i=1}^{k_1+\cdots+k_{j-1}} \mathbb{O}(x_i))^{k_j}$ of $\mathbb{S}^{k_j}$ for which the overlap graph $\mathcal{H}_{k_j}(x^{(j)})$ is connected while avoiding the overlap regions of the points $x_1, \ldots, x_{k_1+\cdots+k_{j-1}}$.

Write $dx^{(j)} = dx_{k_1+\cdots+k_{j-1}+1} \ldots dx_{k_1+\cdots+k_j}$ in the natural extension of the notation to the differential. It then follows that

$$J_{k_1,\ldots,k_\gamma} = \frac{k!}{k_1!\ldots k_\gamma!}\frac{1}{\pi^k}\int_{\mathbb{C}_{k_1}^{(1)}} dx^{(1)} \int_{\mathbb{C}_{k_2}^{(2)}} dx^{(2)} \cdots \int_{\mathbb{C}_{k_\gamma}^{(\gamma)}} dx^{(\gamma)} \mathbf{P}\left({}^0L_{1,\ldots,k}(t) \,|\, X_1 = x_1, \ldots, X_k = x_k\right)$$

Now arguing as in (20), we obtain the bound

$$\mathbf{P}\left({}^0L_{1,\ldots,k}(t) \,|\, X_1 = x_1, \ldots, X_k = x_k\right) \leq \left[1 + \mathcal{O}\left(\frac{\log^2 n}{n}\right)\right] e^{-na_k(x_1,\ldots,x_k)G(t)}$$

where, for each k-tuple $(x_1, \ldots, x_k)$ in $\mathbb{C}_{k_1,\ldots,k_\gamma}$, we have

$$a_k(x_1,\ldots,x_k) = a_{k_1}\left(x^{(1)}\right) + a_{k_2}\left(x^{(2)}\right) + a_{k_3}\left(x^{(3)}\right) + \cdots + a_{k_\gamma}\left(x^{(\gamma)}\right)$$

as the visibility regions across components do not overlap. It then follows that

$$\begin{aligned} J_{k_1,\ldots,k_\gamma} \leq \left[1 + \mathcal{O}\left(\frac{\log^2 n}{n}\right)\right] \frac{k!}{k_1!\ldots k_\gamma!} &\times \frac{1}{\pi^{k_1}} \int_{\mathbb{C}_{k_1}^{(1)}} dx^{(1)} e^{-na_{k_1}(x^{(1)})G(t)} \\ &\times \frac{1}{\pi^{k_2}} \int_{\mathbb{C}_{k_2}^{(2)}} dx^{(2)} e^{-na_{k_2}(x^{(2)})G(t)} \cdots \\ &\times \frac{1}{\pi^{k_\gamma}} \int_{\mathbb{C}_{k_\gamma}^{(\gamma)}} dx^{(\gamma)} e^{-na_{k_\gamma}(x^{(\gamma)})G(t)}. \end{aligned} \quad (33)$$

A typical nested integral on the right-hand side is of the form

$$\begin{aligned} &\frac{1}{\pi^{k_j}} \int_{\mathbb{C}_{k_j}^{(j)}} dx^{(j)} e^{-na_{k_j}(x^{(j)})G(t)} \\ &= \mathbf{E}\left[1_{\mathbb{C}_{k_j}^{(j)}}\left(X^{(j)}\right) e^{-na_{k_j}(X^{(j)})G(t)} \,\middle|\, X_1 = x_1, \ldots, X_{k_1+\cdots+k_{j-1}} = x_{k_1+\cdots+k_{j-1}}\right] \end{aligned} \quad (34)$$

and exhibits one of two distinct behaviors depending on the value of k_j. If $k_j = 1$ (that is the jth component consists of a singleton point) then as per our earlier calculations in (10) the integral differs from λ/n only by a multiplicative term $1+\mathfrak{o}(1)$ as $\mathbb{C}_{k_j}^{(j)}$ differs from $\mathbb{S}^{k_j} = \mathbb{S}$ only in a region $\bigcup_{i=1}^{k_1+\cdots+k_{j-1}} \mathbb{O}(x_i)$ whose area is of order $\mathcal{O}(r^2)$. If $k_j \geq 2$, on the other hand, then the integral is bounded above by

$$\mathbf{E}\left[1_{\mathbb{C}_{k_j}}\left(X^{(j)}\right) e^{-na_{k_j}(X^{(j)})G(t)}\right]$$

as $\mathbb{C}_{k_j}^{(j)} \subset \mathbb{C}_{k_j}$ and the set $\mathbb{C}_{k_j}$ is independent of $X_1, \ldots, X_{k_1+\cdots+k_{j-1}}$. But the last equation differs only notationally in the replacement of k by k_j from the expectation on the right-hand side of the bound (21) for J_k. The results of our analysis for connected overlap graphs hence carries over *in toto* and, as per the estimate (32), the integral (34) is asymptotically $\mathfrak{o}(n^{-k_j})$.

Suppose now that there are exactly j components, say $i_1, \ldots, i_j$, each of which consists of two or more vertices with the remaining $\gamma - j$ components being singletons. Bear in mind that $j \geq 1$ as $\gamma < k$ so that there is at least one nonsingleton component. Clearly, also, $k_{i_1} + \cdots + k_{i_j} = k - \gamma + j$. Each of the $\gamma - j$ singleton components contributes a multiplicative factor of $\frac{\lambda}{n}(1 + \mathfrak{o}(1))$ to the right-hand side of (33) so that the cumulative multiplicative contribution of the singleton components to the expression for $J_{k_1,\ldots,k_\gamma}$ is $\frac{\lambda^{\gamma-j}}{n^{\gamma-j}}(1 + \mathfrak{o}(1))$. On the other hand, the $j \geq 1$ nonsingleton components contribute multiplicative factors of $\mathfrak{o}(n^{-k_{i_1}}), \ldots, \mathfrak{o}(n^{-k_{i_j}})$, respectively, for a cumulative multiplicative factor of $\mathfrak{o}(n^{-(k_{i_1}+\cdots+k_{i_j})})$. Putting both terms together we obtain the asymptotic estimate

$$J_{k_1,\ldots,k_\gamma} = \mathfrak{o}\left(\frac{1}{n^{k_{i_1}+\cdots+k_{i_j}}} \times \frac{1}{n^{\gamma-j}}\right) \qquad (n \to \infty).$$

Thus each of the summands in the expression for J_{overlap} is $\mathfrak{o}(n^{-k})$ and as the sum ranges over only a bounded number of terms we conclude that $J_{\text{overlap}} = \mathfrak{o}(n^{-k})$ as well. □

REFERENCES

[1] A. Chandrakasan, R. Amirtharajah, S. Cho, J. Goodman, G. Konduri, J. Kulik, W. Rabiner, and A. Wang, "Design considerations for distributed microsensor systems," in *Proc. IEEE 1999 Custom Integr. Circuits Conf. (CICC)*, May 1999, pp. 279–286.

[2] L. P. Clare, G. Pottie, and J. Agre, "Self-organizing distributed sensor networks," in *Proc. SPIE Conf. Unattended Ground Sensor Technol. Appl.*, Apr. 1999, pp. 229–237.

[3] M. Dong, K. Yung, and W. Kaiser, "Low power signal processing architectures for network microsensors," in *Proc. 1997 Int. Symp. Low Power Electron. Design*, Aug. 1997, pp. 173–177.

[4] P. Erdös and A. Renyi, "On the evolution of random graphs," *Magyar Tud. Akad. Mat. Kut. Int. Kozl.*, vol. 5, pp. 17–61, 1960.

[5] W. Feller, *An Introduction to Probability Theory and Its Applications*. New York: Wiley, 1965, vol. I.

[6] M. Francheschetti, private communication.

[7] P. Gupta and P. R. Kumar, "Critical power for asymptotic connectivity in wireless networks," *Stoch. Anal., Contr., Optim. Appl.*, ser. A Volume in Honor of W. H. Fleming, pp. 547–566, 1998.

[8] P. Hall, *Introduction to the Theory of Coverage Processes*. New York: Wiley, 1988.

[9] J. Karamata, "Sur un mode de croissance regulière," *Mathematica (Cluj)*, vol. 4, pp. 38–53, 1930.

[10] S. S. Kunniyur and S. S. Venkatesh, "Network devolution and the growth of sensory lacunae in sensor networks," in *Proc. WiOpt'04: Modeling and Optim. Mobile, Ad Hoc Wireless Netw.*, Cambridge, U.K., Mar. 2004, Univ. Cambridge.

[11] S. S. Kunniyur and S. S. Venkatesh, "Sensor network devolution and breakdown in survivor connectivity," in *Proc. 2004 Int. Symp. Inf. Theory*, Chicago, IL, Jun. 27–Jul. 2 2004.

[12] R. Meester and R. Roy, *Continuum Percolation*. Cambridge, U.K.: Cambridge University Press, 1996.

[13] M. Penrose, "The longest edge of the random minimal spanning tree," *Ann. Appl. Prob.*, vol. 7, pp. 340–361, 1997.

[14] M. Penrose, *Random Geometric Graphs*. Cambridge, U.K.: Oxford University Press, 2003.

[15] S. Shakkottai, R. Srikant, and N. Shroff, "Unreliable sensor grids: coverage, connectivity and diameter," in *Proc. IEEE INFOCOM*, San Francisco, CA, 2003.

[16] Connectivity in Geometric Random Graphs 2004 [Online]. Available: http://www.seas.upenn.edu/~venkates/publications_new.html, S. S. Venkatesh, preprint

[17] S. S. Venkatesh, "Connectivity, devolution, and lacunae in geometric random digraphs," in *Proc. Inaug. Worksh. Inf. Theory Appl.*, San Diego, CA, Feb. 2006 [Online]. Available: http://ita.ucsd.edu/workshop/papers/165.pdf

[18] C.-W. Yi, P.-J. Wan, X.-Y. Li, and O. Frieder, "Fault tolerant sensor networks with Bernoulli nodes," in *Proc. IEEE Wireless Commun. Networking Conf. (WCNC)*, New Orleans, LA, Mar. 2003.